SANDIA REPORT

SAND96-0583 • UC-700 Unlimited Release Printed March 1996

Accuracy Considerations for Implementing Velocity Boundary Conditions in Vorticity Formulations

RECEIVED

JUN 0 3 1996

OSTI

S. N. Kempka, M. W. Glass, J.S. Peery, J. H. Strickland



Issued by Sandia National Laboratories, operated for the United States Department of Energy by Sandia Corporation.

NOTICE: This report was prepared as an account of work sponsored by an agency of the United States Government. Neither the United States Government nor any agency thereof, nor any of their employees, nor any of their contractors, subcontractors, or their employees, makes any warranty, express or implied, or assumes any legal liability or responsibility for the accuracy, completeness, or usefulness of any information, apparatus, product, or process disclosed, or represents that its use would not infringe privately owned rights. Reference herein to any specific commercial product, process, or service by trade name, trademark, manufacturer, or otherwise, does not necessarily constitute or imply its endorsement, recommendation, or favoring by the United States Government, any agency thereof or any of their contractors or subcontractors. The views and opinions expressed herein do not necessarily state or reflect those of the United States Government, any agency thereof or any of their contractors.

Printed in the United States of America. This report has been reproduced directly from the best available copy.

Available to DOE and DOE contractors from Office of Scientific and Technical Information PO Box 62 Oak Ridge, TN 37831

Prices available from (615) 576-8401, FTS 626-8401

Available to the public from
National Technical Information Service
US Department of Commerce
5285 Port Royal Rd
Springfield, VA 22161

NTIS price codes Printed copy: A04 Microfiche copy: A01

DISCLAIMER

This report was prepared as an account of work sponsored by an agency of the United States Government. Neither the United States Government nor any agency thereof, nor any of their employees, makes any warranty, express or implied, or assumes any legal liability or responsibility for the accuracy, completeness, or usefulness of any information, apparatus, product, or process disclosed, or represents that its use would not infringe privately owned rights. Reference herein to any specific commercial product, process, or service by trade name, trademark, manufacturer, or otherwise does not necessarily constitute or imply its endorsement, recommendation, or favoring by the United States Government or any agency thereof. The views and opinions of authors expressed herein do not necessarily state or reflect those of the United States Government or any agency thereof.

DISCLAIMER

Portions of this document may be illegible in electronic image products. Images are produced from the best available original document.

Accuracy Considerations for Implementing Velocity Boundary Conditions in Vorticity Formulations

S.N. Kempka, M.W. Glass, J.S. Peery, J.H. Strickland Engineering Sciences Center Sandia National Laboratories Albuquerque, NM 87185

> M.S. Ingber University of New Mexico Albuquerque, NM 87131

Abstract

A vorticity formulation is described that satisfies velocity boundary conditions for the incompressible Navier-Stokes equations. As in previous methods, velocity boundary conditions are satisfied by determining the appropriate vortex sheets that must be created on the boundary. Typically, the vortex sheet strengths are determined by solving a set of linear equations that is over-specified. The over-specification arises because an integral constraint on the vortex sheets is imposed. Vortex sheets determined this way do not accurately satisfy both components of the velocity boundary conditions because over-specified systems do not have unique solutions. To avoid this over-specification and more accurately satisfy velocity boundary conditions, an integral collocation technique is applied to a generalized Helmholtz' decomposition. This formulation implicitly satisfies an integral constraint that is more general than constraints typically used. Improvements in satisfying velocity boundary conditions are shown.

This page is intentionally blank.

Acknowledgments

This work was funded under Laboratory Directed Research and Development (LDRD) and Engineering Science Research Foundation (ESRF) programs and at SNL. The authors thank Wahid Hermina for suggesting that we undertake the proof in Appendix B, which provided additional confidence in the validity of the generalized Helmholtz decomposition. We also thank Mark Christon and P. Randall Schunk for reviewing this report.

Accuracy Considerations for Implementing Velocity Boundary Conditions in Vorticity Formulations

Introduction	9
Analytical Formulation	13
1. Numerical Formulation	17
2. Accuracy Assessment	21
Summary	25
APPENDIX A Construction of a Generalized Helmholtz Decomposition	29
Derivation of the Generalized Helmholtz Decomposition Vortex Sheets	32
2.2 Source Sheets	
APPENDIX B: Validation of a Generalized Potential Velocity Field	39
References	47

Introduction

The satisfaction of velocity boundary conditions in vorticity formulations is examined in detail. Our objective is to develop numerical methods to satisfy velocity boundary conditions more accurately than previous formulations. In previous formulations, errors in satisfying velocity boundary conditions are typically much larger than numerical round off errors. The main source of errors in satisfying velocity boundary conditions is that, as stated by Ostrikov and Zhmulin [30], "we can say with confidence that the analytic theory of vortex dynamics of a viscous fluid is not yet formulated." Accurately satisfying velocity boundary conditions is particularly important in analyses where stability is a concern, or where flow separation occurs (which strongly influences drag). In analyses of these types, boundary conditions must be satisfied accurately to have confidence in the solutions. Moreover, engineers who use primitive variable computational fluid dynamics are accustomed to satisfying velocity boundary conditions to within round off error. Accordingly, they are not generally motivated to make use of formulations (vorticity, or otherwise) that satisfy boundary conditions less accurately, in spite of advantages that the other methods offer. Thus, we seek to formulate an improved theory and numerical method to satisfy velocity boundary conditions, and to assess its accuracy in detail.

The principal feature missing from the analytic theory of viscous vortex dynamics is a formulation to uniquely describe the generation of vorticity that is necessary to satisfy velocity boundary conditions whenever the tangential velocity boundary condition is specified [30]. The difficulty is that vorticity is the dependent variable in vorticity formulations, so that velocity boundary conditions must somehow be represented in terms of vorticity. What is known is that the Navier-Stokes equations indicate that, in order to satisfy tangential velocity boundary conditions, vorticity must be created at the boundary (Batchelor [3]). Neither boundary vorticity nor its flux is generally known a priori, however, and as a result, additional equations must be introduced to relate velocity boundary conditions to vorticity creation.

Many vorticity boundary condition schemes have been proposed, comprising a wide range of different approaches (e.g., streamfunction-vorticity (Roache [35], Parmentier and Torrance [31], and Quartapelle [33], [34], Anderson [1], Koumoutsokos, et al. [19], [20]), velocity-vorticity Cauchy formulation (Gatski et al. [9]), vorticity-velocity Poisson equation (Daube [8]), Biot-Savart (Chorin and Marsden [7]), generalized Helmholtz decomposition (Wu (J. C.) [39], [40], [41], [42], (also in [4]), Morino [27], [28], Uhlman et al. [37]). The above formulations rely on kinematics to describe vorticity creation. Other approaches use dynamics (the Navier-Stokes equations) on the boundary (Kinney et al. [16], [13], Wu (J.-Z.) [43]). See also reviews by Gresho [10], Puckett [32], Leonard [21], [22], Sarpkaya [36].

Various features which remain unresolved regarding vorticity creation are:

- Is there a unique specification of vorticity flux to satisfy velocity boundary conditions? (Some Unanswered Questions in Fluid Mechanics [23].)

- What are the proper integral constraints on vorticity created on boundaries? And, how should they be implemented in a numerical formulation? (Typically, an integral constraint is imposed on a linear set of equations for vortex sheets on the boundary, to yield an overspecified set of equations. There are several methods to solve over-specified systems of equations (e.g., Hess [11], [12]), but the solution is not unique; (i.e., the solution depends on the type of solution method used), and the methods rely mainly on empirical criteria, as discussed by Koumoutsokos [18]. Koumoutsokos developed a method to incorporate a constraint without over-specifying the system for a stream function formulation. We seek a formulation that does not require the use of streamfunctions.
- Should both normal and tangential components of the velocity boundary condition be imposed? Or, is it sufficient to impose only one component? If so, how is it that the unspecified component is satisfied?
- Are kinematics sufficient to specify vorticity creation? Or, must dynamic information be used?
- Is the value of vorticity on the boundary (Dirichlet) or its normal gradient (von Neumann) the appropriate vorticity boundary condition?

A more pragmatic view of the problem can be seen by considering a typical time step in a numerical solution of the vorticity transport equation. Assume a vorticity field exists that satisfies the velocity boundary conditions. The vorticity field is then transported according to the vorticity form of the Navier-Stokes equation, wherein vorticity is convected by the velocity field and diffused as a result of the fluid viscosity. Diffusion of vorticity from the boundary into the domain, and its convective transport are omitted during the time step due to a lack of a vorticity boundary condition. The omitted vorticity and the rest of the vorticity field would induce motion that would satisfy the velocity boundary condition. But, since some vorticity is missing, the velocity boundary conditions are not satisfied. Thus, the vorticity field adjacent to the boundary must be corrected.

With the understanding that the vorticity field adjacent to the boundary is deficient, a vorticity boundary condition is seen to be an artifice to introduce the desired correction to the vorticity in the domain. A Neumann boundary condition specifies a unique addition of vorticity to the domain, independent of the existing vorticity field (since diffusion can be separated into two problems: a homogeneous von Neumann boundary condition with an inhomogeneous initial condition, and an inhomogeneous von Neumann boundary condition with a homogeneous initial condition). A Dirichlet boundary condition can also specify a unique addition of vorticity to the domain, but it depends on the existing vorticity field, which is less convenient. Typically, the correction for the vorticity field is found in terms of a zero-thickness vortex sheet (Lighthill [24]), which is assumed to expand by viscous diffusion to a finite thickness layer of finite vorticity. A unique specification of the vorticity gradient can be defined from vortex sheets (Koumoutsakos [19], Kempka, et al. [15]) contrary to statements made by Wu [43].

The aforementioned unresolved issues lead to errors in satisfying velocity boundary conditions. In many previous schemes, only one component of the velocity boundary condi-

tion is satisfied at a time; *i.e.*, both components are not satisfied simultaneously. Other schemes simply do not satisfy the tangential velocity boundary condition (*e.g.*, Roache [35]). In most cases, the accuracy to which boundary conditions are satisfied is not discussed in detail.

The investigation by Uhlman et al. [37] is a notable exception. They consider the flow of an otherwise uniform freestream around a solid, impermeable cylinder in which there is no other vorticity in the flow field. The no-slip (zero tangential velocity) boundary condition is satisfied (at collocation points) by determining a vortex sheet strength on the surface. The normal velocity is not satisfied as accurately, however, and they describe the convergence of the normal velocity boundary condition with discretization of the boundary.

We consider the convergence of the velocity boundary conditions in the presence of a non-zero vorticity field. We show that the need for integral constraints arises from non-zero vorticity fields. Failure to accurately satisfy integral constraints is shown to relate directly to errors in satisfying the velocity boundary conditions. We also note that the constraints used in previous analyses are not appropriate for general flows. We present an analytical formulation that implicitly satisfies a necessary integral constraint on the vorticity field. The constraint is applicable to all flows. A numerical method to solve the system is presented which is designed to satisfy the constraint implicitly for all discretizations, thus providing a well-posed method for general flows. Boundary velocities are shown to converge faster than previous formulations.

Analytical Formulation

The vorticity form of the Navier-Stokes equations for an incompressible flow is

$$\frac{\partial \underline{\omega}}{\partial t} + (\underline{u} \bullet \nabla)\underline{\omega} = (\underline{\omega} \bullet \nabla)\underline{u} + \nu \nabla^2\underline{\omega} , \qquad (1)$$

where the velocity field \underline{u} , the vorticity is $\underline{\omega} = \nabla \times \underline{u}$, t is time, the constant fluid density is ρ , the constant kinematic fluid viscosity is ν , and ∇ is the gradient operator.

Boundary conditions are often given in terms of the velocity $\underline{u} = \underline{u}_b$ on the boundary S. Specification of a tangential velocity boundary condition generally implies the creation of vorticity on the boundary that must be determined. In addition, the velocity field must be obtained using the vorticity field. The formulation described below determines both vorticity creation and the velocity field in a unified manner.

The velocity field is obtained from the vorticity field and the velocity boundary conditions using a generalized Helmholtz' decomposition (GHD). The GHD can be viewed as the infinite domain solution to the vector Poisson equation

$$\nabla^2 u = -\nabla \times \omega + \nabla D \tag{2}$$

obtained by performing the curl operation on the definition of vorticity $\omega = \nabla \times \underline{u}$, with $D = \nabla \bullet \underline{u}$.

The GHD has been derived independently by several investigators including Wu and Thompson [39], Morino [27] (based on work by Bykhovskiy and Smirnov [5]), Uhlman and Grant [37] (based on work by Morse and Feshback [29]), and Meir and Schmidt [25] (none of whom reference one another, except Morino, who briefly notes some of Wu's work). (A derivation of the GHD is found in Appendix A.)

For the velocity boundary condition $u = u_b$ on the boundary S, and denoting the fluid domain as R, the GHD is

$$\begin{cases}
0 \text{ outside } R \text{ and } S \\
\alpha 2\pi (d-1) \underline{u}_b^*(\underline{x}) \text{ on } S \\
2\pi (d-1) \underline{u}(\underline{x}) \text{ in } R
\end{cases} =$$
(3)

$$\int_{R} \frac{\underline{\omega}^{*}(\underline{x}') \times (\underline{x} - \underline{x}')}{|\underline{x} - \underline{x}'|^{d}} dR(\underline{x}') + \int_{S} \frac{[-\hat{n}(\underline{x}_{b}') \times \underline{u}_{b}^{*}(\underline{x}_{b}')] \times (\underline{x} - \underline{x}')}{|\underline{x} - \underline{x}'|^{d}} dS(\underline{x}_{b}') +$$

$$\int_{R} \frac{D(\underline{x}')(\underline{x}-\underline{x}')}{|\underline{x}-\underline{x}'|^{\mathrm{d}}} dR(\underline{x}') + \int_{S} \frac{-[\hat{n}(\underline{x}_{b}') \bullet \underline{u}_{b}^{*}(\underline{x}_{b}')](\underline{x}-\underline{x}')}{|\underline{x}-\underline{x}'|^{\mathrm{d}}} dS(\underline{x}_{b}')$$

In Eq. (3), x is a point in the infinite domain, primes denote variables of integration, and subscript "b" denotes a quantity on the boundary. For two-dimensional flows, d = 2, and for three-dimensional flows, d = 3. The unit normal vector on the boundary (pointing away from the fluid) is \hat{n} .

 α is representative of the internal angle of the boundary divided by 2π (d-1); on smooth boundaries is $\alpha = 1/2$. The superscript * in Eq. (3) denotes that the vorticity field ω and the velocity boundary conditions u_b are kinematically consistent for incompressible flows. The concept of kinematic consistency will be discussed further.

Note that both component of the velocity boundary condition are included in Eq. (3). One boundary integral contains the normal velocity boundary condition $\hat{n} \cdot \underline{u}_b$, and the other contains the tangential velocity boundary conditions in the coefficient $\hat{n} \times \underline{u}_b$.

Although the GHD is valid for compressible flows $(D = \nabla \cdot \underline{u} \neq 0)$, we will consider only incompressible flows; i.e., D = 0.

As mentioned previously, the superscript * in Eq. (3) denotes that the vorticity field ω and the velocity boundary conditions u_b are kinematically consistent. The test for kinematic consistency is that ω and u_b satisfy the boundary form of Eq. (3), which we write in normal and tangential components as

$$\alpha 2\pi (d-1)[\hat{n}(\underline{x}_{b}) \times \underline{u}_{b}^{*}(\underline{x}_{b}) \times \hat{n}(\underline{x}_{b}) + \hat{n}(\underline{x}_{b})(\hat{n}(\underline{x}_{b}) \bullet \underline{u}_{b}^{*})] =$$

$$\int_{R} \frac{\underline{\omega}^{*}(\underline{x}') \times (\underline{x} - \underline{x}')}{|\underline{x} - \underline{x}'|^{d}} dR(\underline{x}') + \int_{S(\underline{x}_{b}' \neq \underline{x}_{b})} \frac{[-\hat{n}(\underline{x}_{b}') \times \underline{u}_{b}^{*}(\underline{x}_{b}')] \times (\underline{x} - \underline{x}')}{|\underline{x} - \underline{x}'|^{d}} dS(\underline{x}_{b}') +$$

$$\int_{R} \frac{D(\underline{x}')(\underline{x} - \underline{x}')}{|\underline{x} - \underline{x}'|^{d}} dR(\underline{x}') + \int_{S(\underline{x}_{b}' \neq \underline{x}_{b})} \frac{-[\hat{n}(\underline{x}_{b}') \bullet \underline{u}_{b}^{*}(\underline{x}_{b}')](\underline{x} - \underline{x}')}{|\underline{x} - \underline{x}'|^{d}} dS(\underline{x}_{b}')$$

$$(4)$$

That is, ω and u_b cannot be specified arbitrarily; in order for ω and u_b to be kinematically consistent, ω and u_b must satisfy Eq. (4).

The need to consider kinematic consistency arises from the specification of a tangential velocity boundary condition. An arbitrary tangential velocity boundary condition cannot be satisfied, in general, for an arbitrary vorticity field. This can be seen from the theorem of the rotational [17],

$$\int \nabla \times u dR = \int \omega dR = \int \hat{n} \times u_b dS.$$

In order to satisfy a tangential velocity boundary condition (and attain kinematic consistency), vorticity generally must be generated at the boundary.

Note that any normal velocity boundary condition can be satisfied for any vorticity field, as long as

$$\int \nabla \bullet u dR = 0 = \int \hat{n} \bullet u_b dS,$$

for incompressible flows (according to the divergence theorem).

Next, we discuss how kinematically *inconsistent* ω and u_b can occur, and how to create the vorticity necessary to obtain kinematic consistency.

Kinematically inconsistent ω and u_b occur during numerical simulations in which explicit time integration is used to advance time for the Navier-Stokes equations. Consider a kinematically consistent initial condition for ω and u_b . As the vorticity field is transported according to the Navier-Stokes equations, production and transport of vorticity at the boundary is not generally accounted for, because the proper boundary condition is not known. As a result, the new ω and u_b are no longer kinematically consistent; *i.e.*, Eq. (4) is not generally satisfied, and vorticity must be generated on the boundary.

Lighthill [24] proposed that the circulation associated with the unaccounted for vorticity field could be represented by a vortex sheet. Conveniently enough, the boundary integrals in Eq. (3) represent the motion induced by vortex sheets γ and source sheets σ , with strengths $\gamma = -\hat{n} \times \underline{u}_b$ and $\sigma = -\hat{n} \cdot \underline{u}_b$. (see Appendix A for further details.)

Following Lighthill's approach, if the vortex sheet representing the circulation generated on the boundary is denoted as $\underline{\gamma}_c$, we can write an equation that is valid for arbitrary $\underline{\omega}$ and \underline{u}_b , subject to the determination of $\underline{\gamma}_c$.

$$\begin{cases}
0 \text{ outside } R \text{ and } S \\
\alpha(\underline{x}_b)2\pi(d-1)[\underline{u}_b(\underline{x}_b) - \underline{\gamma}_c(\underline{x}_b) \times \hat{n}(\underline{x}_b)] \text{ on } S \\
2\pi(d-1)\underline{u}(\underline{x}) \text{ in } R
\end{cases} =$$
(5)

$$\int_{R} \frac{\underline{\omega}(\underline{x}') \times (\underline{x} - \underline{x}')}{|\underline{x} - \underline{x}'|^{\mathrm{d}}} dR(\underline{x}') + \int_{S} \frac{[\underline{\gamma}_{c}(\underline{x}_{b}') - \hat{n}(\underline{x}_{b}') \times \underline{u}_{b}(\underline{x}_{b}')] \times (\underline{x} - \underline{x}')}{|\underline{x} - \underline{x}'|^{\mathrm{d}}} dS(\underline{x}_{b}') + \frac{1}{2} \int_{S} \frac{[\underline{\gamma}_{c}(\underline{x}_{b}') - \hat{n}(\underline{x}_{b}') \times \underline{u}_{b}(\underline{x}_{b}')] \times (\underline{x} - \underline{x}')}{|\underline{x} - \underline{x}'|^{\mathrm{d}}} dS(\underline{x}_{b}') + \frac{1}{2} \int_{S} \frac{[\underline{\gamma}_{c}(\underline{x}_{b}') - \hat{n}(\underline{x}_{b}') \times \underline{u}_{b}(\underline{x}_{b}')] \times (\underline{x} - \underline{x}')}{|\underline{x} - \underline{x}'|^{\mathrm{d}}} dS(\underline{x}_{b}') + \frac{1}{2} \int_{S} \frac{[\underline{\gamma}_{c}(\underline{x}_{b}') - \hat{n}(\underline{x}_{b}') \times \underline{u}_{b}(\underline{x}_{b}')] \times (\underline{x} - \underline{x}')}{|\underline{x} - \underline{x}'|^{\mathrm{d}}} dS(\underline{x}_{b}') + \frac{1}{2} \int_{S} \frac{[\underline{\gamma}_{c}(\underline{x}_{b}') - \hat{n}(\underline{x}_{b}') \times \underline{u}_{b}(\underline{x}_{b}')] \times (\underline{x} - \underline{x}')}{|\underline{x} - \underline{x}'|^{\mathrm{d}}} dS(\underline{x}_{b}') + \frac{1}{2} \int_{S} \frac{[\underline{\gamma}_{c}(\underline{x}_{b}') - \hat{n}(\underline{x}_{b}') \times \underline{u}_{b}(\underline{x}_{b}')] \times (\underline{x} - \underline{x}')}{|\underline{x} - \underline{x}'|^{\mathrm{d}}} dS(\underline{x}_{b}') + \frac{1}{2} \int_{S} \frac{[\underline{\gamma}_{c}(\underline{x}_{b}') - \hat{n}(\underline{x}_{b}') \times \underline{u}_{b}(\underline{x}_{b}')] \times (\underline{x} - \underline{x}')}{|\underline{x} - \underline{x}'|^{\mathrm{d}}} dS(\underline{x}_{b}') + \frac{1}{2} \int_{S} \frac{[\underline{\gamma}_{c}(\underline{x}_{b}') - \underline{n}(\underline{x}_{b}') \times \underline{u}_{b}(\underline{x}_{b}')] \times (\underline{x} - \underline{x}')}{|\underline{x} - \underline{x}'|^{\mathrm{d}}} dS(\underline{x}_{b}') + \frac{1}{2} \int_{S} \frac{[\underline{\gamma}_{c}(\underline{x}_{b}') - \underline{n}(\underline{x}_{b}') \times \underline{u}_{b}(\underline{x}_{b}')] \times (\underline{x} - \underline{x}')}{|\underline{x} - \underline{x}'|^{\mathrm{d}}} dS(\underline{x}_{b}') + \frac{1}{2} \int_{S} \frac{[\underline{\gamma}_{c}(\underline{x}_{b}') - \underline{n}(\underline{x}_{b}') \times \underline{u}_{b}(\underline{x}_{b}')]}{|\underline{x} - \underline{x}'|^{\mathrm{d}}} dS(\underline{x}_{b}') + \frac{1}{2} \int_{S} \frac{[\underline{\gamma}_{c}(\underline{x}_{b}') - \underline{n}(\underline{x}_{b}') \times \underline{u}_{b}(\underline{x}_{b}')]}{|\underline{x} - \underline{x}'|^{\mathrm{d}}} dS(\underline{x}_{b}') + \frac{1}{2} \int_{S} \frac{[\underline{\gamma}_{c}(\underline{x}_{b}') - \underline{n}(\underline{x}_{b}') \times \underline{u}_{b}(\underline{x}_{b}')} + \frac{1}{2} \int_{S} \frac{[\underline{\gamma}_{c}(\underline{x}_{b}') - \underline{n}(\underline{x}_{b}') \times \underline{u}_{b}(\underline{x}_{b}')} + \frac{1}{2} \int_{S} \frac{[\underline{\gamma}_{c}(\underline{x}_{b}') - \underline{n}(\underline{x}_{b}') \times \underline{u}_{b}'} + \frac{1}{2} \int_{S} \frac{[\underline{\gamma}_{c}(\underline{x}_{b}') - \underline{u}_{b}'} + \frac{1}{2} \int_{S} \frac{[\underline{\gamma}_{c}(\underline{x}_{b}') - \underline{u}_{b}']}{|\underline{x} - \underline{x}'|^{\mathrm{d}}} + \frac{1}{2} \int_{S} \frac{[\underline{\gamma}_{c}(\underline{x}_{b}') - \underline{u}_{b}']}{|\underline{x} - \underline{x}'|^{\mathrm{d}}} + \frac{1}{2} \int_{S} \frac{[\underline{\gamma}_{c}(\underline{x}_{b}') - \underline{u}_{b}']}{|\underline{x} - \underline{x}'|^{\mathrm{d}}} + \frac{1}{2} \int_{S} \frac{[\underline$$

$$\int_{R} \frac{D(\underline{x}')(\underline{x}-\underline{x}')}{|\underline{x}-\underline{x}'|^{\mathrm{d}}} dR(\underline{x}') + \int_{S} \frac{-[\hat{n}(\underline{x}_{b}') \bullet \underline{u}_{b}(\underline{x}_{b}')](\underline{x}-\underline{x}')}{|\underline{x}-\underline{x}'|^{\mathrm{d}}} dS(\underline{x}_{b}')$$

The boundary form of this equation, in normal and tangential components on the boundary, is

$$\alpha 2\pi (d-1)\{[\hat{n} \times \underline{u}_b - \gamma_c] \times \hat{n} + \hat{n}[\hat{n} \bullet \underline{u}_b]\} =$$
(6)

$$\int_{R} \frac{\underline{\omega}(\underline{x}') \times (\underline{x} - \underline{x}')}{|\underline{x} - \underline{x}'|^{d}} dR(\underline{x}') + \int_{S(\underline{x}_{b}' \neq \underline{x}_{b})} \frac{[\underline{\gamma}_{c}(\underline{x}_{b}') - \hat{n}(\underline{x}_{b}') \times \underline{u}_{b}(\underline{x}_{b}')] \times (\underline{x} - \underline{x}')}{|\underline{x} - \underline{x}'|^{d}} dS(\underline{x}_{b}') +$$

$$\int_{R} \frac{D(\underline{x}')(\underline{x}-\underline{x}')}{|\underline{x}-\underline{x}'|^{\mathrm{d}}} dR(\underline{x}') + \int_{S(\underline{x}_b'\neq\underline{x}_b)} \frac{-[\hat{n}(\underline{x}_b')\bullet\underline{u}_b(\underline{x}_b')](\underline{x}-\underline{x}')}{|\underline{x}-\underline{x}'|^{\mathrm{d}}} dS(\underline{x}_b')$$

As described at the end of Appendix A, if either the normal or tangential component of Eq. (6) is satisfied, then the other component will also be satisfied. Thus, only one component of Eq. (6) should be specified. To determine which component should be specified, consider that for unknown γ_c , the normal component of Eq. (6) is a Fredholm equation of the first kind, for which $\gamma_c(x_b)$ has zero local contribution to the normal velocity at x_b . Such equations can exhibit poor numerical behavior. The tangential component of Eq. (6) is a Fredholm equation of the second kind, in which the local value of $\gamma_c(x_b)$ has a strong non-zero contribution at x_b , which is $\hat{n} \times \gamma_c \alpha 2\pi(d-1)$, yielding a diagonally dominant matrix. These considerations indicate that it is better to specify the tangential component of the velocity boundary condition.

It is significant to note that Eq. (3) and Eq. (6) satisfy the integral identities

$$\int_{R} (\nabla \times \underline{u}) dR = \int_{S} (\hat{n} \times \underline{u}) dS \quad \text{(the theorem of the rotational [17])}. \tag{7}$$

In the fluid domain, $\nabla \times \underline{u} = \underline{\omega}$, and on the boundary, $-\hat{n} \times \underline{u}$ is a vortex sheet strength, as noted above. With these specifications, the theorem of the rotational for the GHD can be shown to be

$$\int_{R} \omega dR = \int_{S} [(\hat{n} \times \underline{u}_{b}) - \underline{\gamma}] dS . \tag{8}$$

Another identity of interest is the divergence theorem,

$$\int_{R} \nabla \bullet \, \underline{u} dR = \int_{S} \hat{n} \bullet \, \underline{u} dS \tag{9}$$

where $\nabla \bullet \underline{u} = D = 0$ in the fluid domain (for incompressible flows) which imposes a constraint on the normal velocity boundary condition.

Two points of interest regarding these identities are, first, Eq. (7) is an integral relationship between ω , γ , $(\hat{n} \times \underline{u})$. Thus, there should be no need to specify any additional integral constraints on γ , although most previous formulations do so. The constraint most often used is

$$\int_{S} \gamma dS = 0 \tag{10}$$

which is appropriate only for certain flows, such as flow around a closed body with $u_b = 0$. It is not appropriate, however, for flows where there is a non-zero tangential velocity boundary condition, such as the lid-driven cavity.

Secondly, since Eq. (7) is implicitly satisfied by the GHD, discrete formulations used to solve the GHD should also implicitly satisfy Eq. (7). This will be discussed further in the next section.

1. Numerical Formulation

The objective of this section is to formulate a method to solve the GHD (Eq. (6)) for vortex sheets on the boundary in which the integral constraint on vorticity and vortex sheets in Eq. (7) is satisfied implicitly for arbitrary discretizations. This follows the philosophy used to construct numerical methods to solve transport equations in which conservation properties of the analytical equations are satisfied implicitly by the numerical formulation for arbitrary discretizations. The relationship between the proposed method and the integral constraint associated with the Fredholm alternative for integrated equations is discussed.

Most numerical methods to solve for the vortex sheets are based on point collocation techniques in which the discrete equations are obtained by evaluating the GHD (or a related formulation) at the midpoint of each boundary element. The proposed method is based on integrating the GHD over each boundary element, rather than evaluating at a single point. The resulting set of equations will be shown to satisfy the integral constraint implicitly, unlike point collocation methods. For the case of irrotational flow ($\omega = 0$), there are many well-developed boundary element methods for which additional integral constraints are not considered, and are apparently not necessary. Thus, issues related to integral constraints appear to arise from the existence of non-zero vorticity. As a result, we will focus on the influence of the velocity field induced by the vorticity field.

To describe the proposed formulation, consider the equation for the GHD on the boundary (Eq. (6)) in which the velocity induced by the vorticity field (the Biot-Savart law) is denoted as

$$\underline{u}_{\omega} = \frac{1}{2\pi(d-1)} \int_{R} \frac{\underline{\omega}(\underline{x}') \times (\underline{x} - \underline{x}')}{|\underline{x} - \underline{x}'|^{d}} dR(\underline{x}'), \tag{11}$$

the motion induced by a vortex sheet is

$$\underline{u}_{\gamma_c} = \frac{1}{2\pi(d-1)} \int_{S}^{\underline{\gamma}_c(\underline{x}_b') \times (\underline{x} - \underline{x}')} \frac{dS(\underline{x}_b')}{|\underline{x} - \underline{x}'|^d} dS(\underline{x}_b')$$
(12)

and an integral operator that is linear in its velocity vector argument is defined as

$$L(\underline{u}) = \frac{1}{2\pi(d-1)} \int_{S} \frac{[-\hat{n}(\underline{x}_{b}') \bullet (\underline{u})](\underline{x} - \underline{x}')}{|\underline{x} - \underline{x}'|^{d}} dS(\underline{x}_{b}') + \frac{1}{2\pi(d-1)} \int_{S} \frac{[-\hat{n}(\underline{x}_{b}') \times (\underline{u})] \times (\underline{x} - \underline{x}')}{|\underline{x} - \underline{x}'|^{d}} dS(\underline{x}_{b}')$$
(13)

In this notation, the GHD becomes

$$\begin{cases}
0 \text{ outside } R \text{ and } S \\
\alpha(\underline{x}_b)[\underline{u}_b(\underline{x}_b) - \underline{\gamma}_c(\underline{x}_b) \times \hat{n}(\underline{x}_b)] \text{ on } S \\
\underline{u}(\underline{x}) \text{ in } R
\end{cases} = \underline{u}_{\omega} + L(\underline{u}_b) + \underline{u}_{\gamma_c} \tag{14}$$

Substituting $L(\underline{u}_b) = L(\underline{u}_\omega) + L(\underline{u}_b - \underline{u}_\omega)$ yields

$$\begin{cases}
0 \text{ outside } R \text{ and } S \\
\alpha(\underline{x}_b)[\underline{u}_b(\underline{x}_b) - \underline{\gamma}_c(\underline{x}_b) \times \hat{n}(\underline{x}_b)] \text{ on } S \\
\underline{u}(\underline{x}) \text{ in } R
\end{cases} = [\underline{u}_{\omega} + L(\underline{u}_{\omega})] + [L(\underline{u}_b - \underline{u}_{\omega}) + \underline{u}_{\gamma_c}] \tag{15}$$

The first bracketed term on the right hand side is a kinematically consistent velocity field in its own right, since $u_{\omega}(x_b)$ is certainly a valid boundary condition for $u_{\omega}(x)$. Following the paradigm of the GHD for kinematically consistent boundary conditions, Eq. (3), for the special case $u_b = u_{\omega}(x_b)$,

$$\begin{cases}
0 \text{ outside } R \text{ and } S \\
\alpha(\underline{x}_b)\underline{u}_{\omega}(\underline{x}_b) \text{ on } S \\
\underline{u}_{\omega}(\underline{x}) \text{ in } R
\end{cases} = \underline{u}_{\omega} + L(\underline{u}_{\omega}) \tag{16}$$

For later use, note that the boundary form of Eq. (16) is,

$$[1-\alpha(\underline{x}_b)]\underline{u}_{\omega} + L(\underline{u}_{\omega}) = 0 \text{ on S.}$$
 (17)

The second bracketed term in Eq. (15) is an incompressible, irrotational velocity field. As described in Batchelor [3] (exercise 2.4), this type of velocity field can be described in terms of a vortex sheet γ_{ϕ} ,

$$\underline{u}_{\gamma_{\phi}} = \frac{1}{2\pi(d-1)} \int_{S}^{\underline{\gamma}_{\phi}(\underline{x}_{b}') \times (\underline{x} - \underline{x}')} \frac{|\underline{x} - \underline{x}'|^{d}}{|\underline{x} - \underline{x}'|^{d}} dS(\underline{x}_{b}') = L(\underline{u}_{b} - \underline{u}_{\omega}) + \underline{u}_{\gamma_{c}}.$$
(18)

With this new representation for $L(\underline{u}_b - \underline{u}_\omega) + \underline{u}_{\gamma_c}$, Eq. (15) becomes

$$\begin{cases}
0 \text{ outside } R \text{ and } S \\
\alpha(\underline{x}_b)[\underline{u}_{\omega}(\underline{x}_b) - \underline{\gamma}_{\phi}(\underline{x}_b) \times \hat{n}(\underline{x}_b)] \text{ on } S \\
\underline{u}(\underline{x}) \text{ in } R
\end{cases} = [\underline{u}_{\omega} + L(\underline{u}_{\omega})] + \underline{u}_{\gamma_{\phi}} \tag{19}$$

The boundary form Eq. (19) can be re-arranged to obtain a vector Fredholm equation,

$$\alpha(\underline{x}_b)[-\underline{\gamma}_{\phi}(\underline{x}_b) \times \hat{n}(\underline{x}_b)] - \frac{1}{2\pi(d-1)} \int_{S} \frac{\underline{\gamma}_{\phi}(\underline{x}_b') \times (\underline{x} - \underline{x}')}{|\underline{x} - \underline{x}'|^{d}} dS(\underline{x}_b') =$$
(20)

$$[1 - \alpha(\underline{x}_b)]\underline{u}_{\omega}(\underline{x}_b) + L(\underline{u}_{\omega}) \, = \, \underline{h}(\underline{x}_b) \, .$$

The tangential component of this vector equation has the canonical form of a Fredholm equation of the second kind. The Fredholm alternative states that in order for a unique solution for Υ_{ϕ} to exist, the tangential component of the right hand side, $h_{\tau}(\underline{x}_b) = \hat{n} \times h(\underline{x}_b) \times \hat{n}$, must satisfy the integral constraint

$$\int_{S} \Psi(\underline{x}') h_{\tau}(\underline{x}') dS(\underline{x}') = 0$$
(21)

where $\psi(x_b)$ represents the eigenfunctions for the adjoint problem, [26].

However, from Eq. (17), $h(x_b) = [1-\alpha(x_b)]u_{\omega}(x_b) + L(u_{\omega}) = 0$; thus the Fredholm constraint is satisfied identically. (Note that if there is no vorticity, the constraint is also satisfied, so that no constraint issues arise for potential flows.)

The above analysis indicates that in order to obtain valid numerical solutions, the numerical representation of $[1-\alpha(\underline{x}_b)]\underline{u}_{\omega}(\underline{x}_b) + L(\underline{u}_{\omega}) = 0$ must be very accurate. This entails accurately calculating the integral of the tangential component Biot-Savart velocity on the boundary. For consistency, all the other boundary integrals must also be accurately resolved, which motivates the proposed integral collocation approach.

To begin, the GHD on the boundary is,

$$\alpha\{[\hat{n} \times \underline{u}_b - \underline{\gamma}_c] \times \hat{n} + \hat{n}[\hat{n} \bullet \underline{u}_b]\} = \underline{u}_\omega + \underline{u}_\gamma + L(\underline{u}_b) . \tag{22}$$

The tangential component is,

$$-\hat{n} \times \underline{u}_{\gamma} \times \hat{n} + \alpha \hat{n} \times \gamma_{c} = \hat{n} \times [-\alpha \underline{u}_{b} + \underline{u}_{\omega} + L(\underline{u}_{b})] \times \hat{n}. \tag{23}$$

(The singular contribution $-\gamma_c \times \hat{n}$ from u_{γ} is written explicitly, whereas the singular contribution to $L(u_h)$ is not written explicitly.)

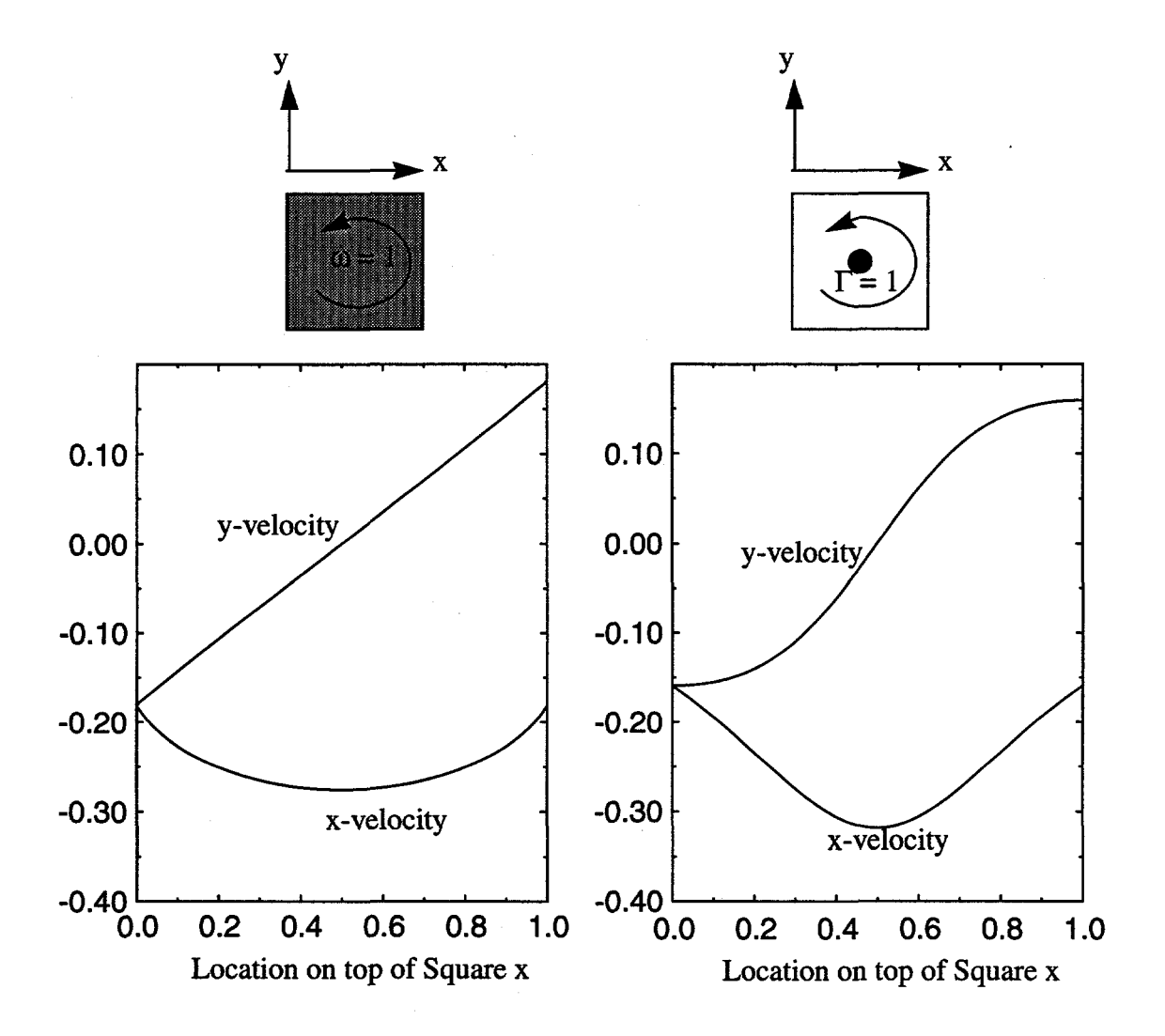


Figure 1 Velocity components induced on the top of the unit square by unit vorticity filling the square, and a point vortex at the center of the square, with unit circulation.

To ensure accurate representation of boundary integrals, Eq. (23) is integrated over each discrete boundary element,

$$\int_{element_{i}} [-\hat{n} \times \underline{u}_{\gamma} \times \hat{n} + \alpha \hat{n} \times \underline{\gamma}_{c}] dS =$$
(24)

$$\int\limits_{element_i} \hat{n}(\underline{x}_b) \times [(-\alpha \underline{u}_b) + \underline{u}_{0} + L(\underline{u}_b)] \times \hat{n}(\underline{x}_b) dS.$$

The left-hand side contains the unknown vortex sheets, and when discretized, yields matrix coefficients for the vortex sheet strengths. The right-hand side contains known quanti-

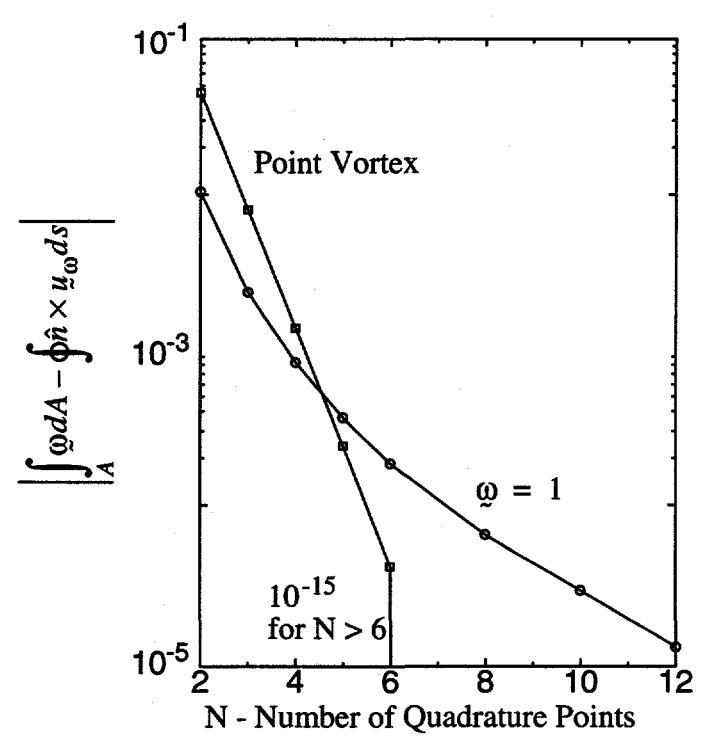


Figure 2 Residual of the theorem of the rotational for 1) unit vorticity in the unit square, and 2) a point vortex with unit circulation at the center of the unit square. Residuals are calculated for N-order Gaussian quadratures.

ties, which allows the vortex sheet strength to be determined by solving the dense linear system of equations.

To see how this formulation accurately satisfies the important boundary integrals containing the velocity induced by the vorticity, u_{ω} , consider the term,

$$\int_{element_i} \hat{n} \times \underline{u}_{\omega} dS. \tag{25}$$

(The magnitude of $\hat{n} \times \underline{u}_{\omega}$ is the same as the magnitude of $\hat{n} \times \underline{u}_{\omega} \times \hat{n}$.) The sum of these terms over all boundary elements is the complete boundary integral of the tangential velocity,

$$\sum_{i=1}^{\text{n_elements}} \int_{element_i} \hat{n} \times \underline{u}_{\omega} dS_i = \int_{S} \hat{n} \times \underline{u}_{\omega} dS$$
 (26)

which we know must satisfy the theorem of the rotational,

$$\int_{R} \omega dR = \int_{S} \hat{n} \times \underline{u}_{\omega} dS. \tag{27}$$

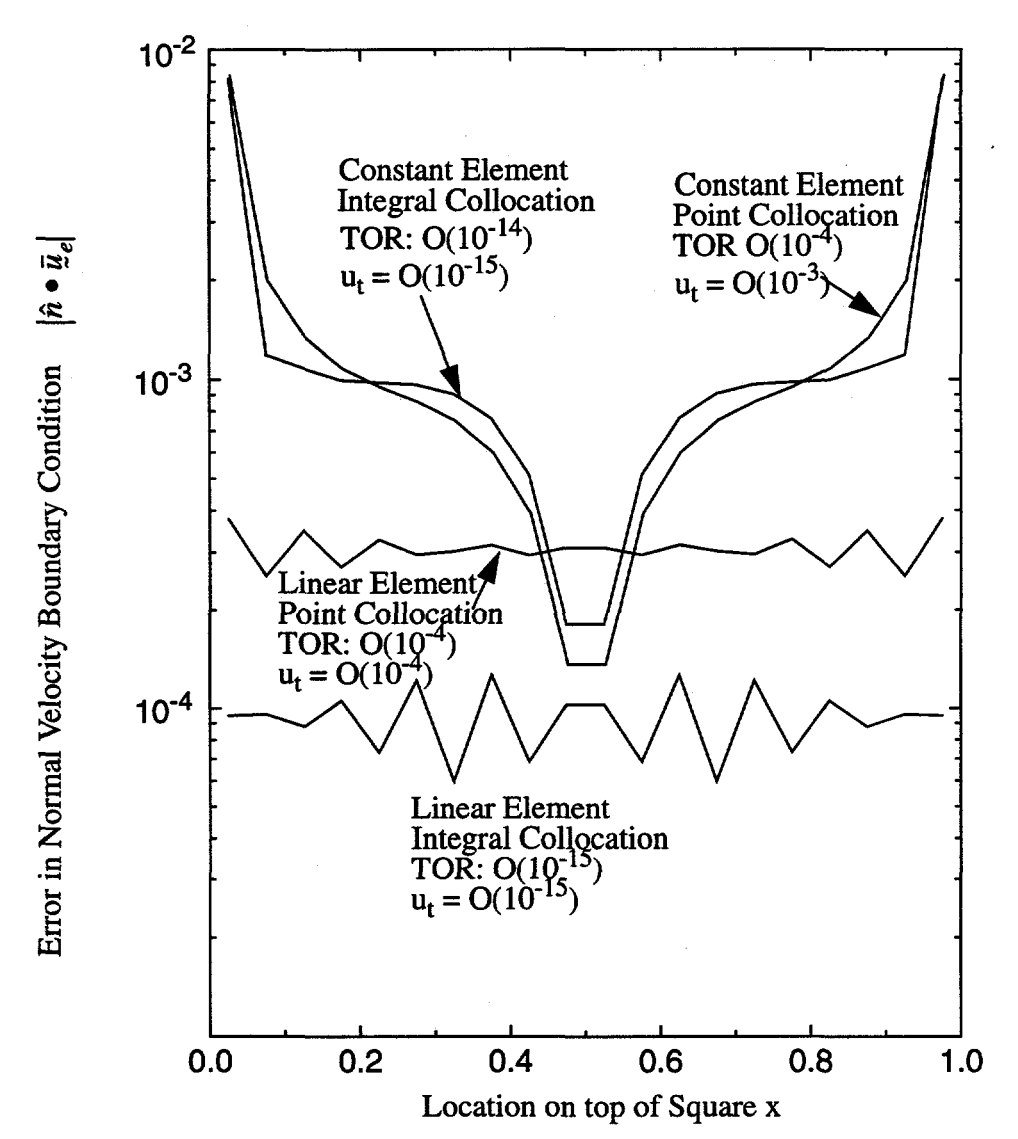


Figure 3 Errors in satisfying the zero velocity boundary condition for a point vortex in the unit square, 20 boundary elements on each side. Errors on one side of the unit square are shown for four solution methods are shown. ut denotes the largest integral error in tangential velocity. TOR denotes the residual to the Theorem of the Rotational.

Thus, the theorem of the rotational provides a measure of how well the boundary integrals are being represented. This provides a paradigm about which the numerical method can be designed. In particular, the numerical method must ensure that the boundary integrals for each element (Eq. (25)) are calculated so their sum satisfies Eq. (27). As will be seen, errors in satisfying Eq. (25) result in errors in satisfying the velocity boundary conditions.

To summarize the proposed approach, the tangential component of the GHD is integrated over each boundary element (integral collocation). The integral of the tangential velocity over each element must be accurately represented, so that collectively, the resulting set of linear equations accurately satisfies the theorem of the rotational. Thus, no additional constraints need to be imposed, so there is no over-specification.

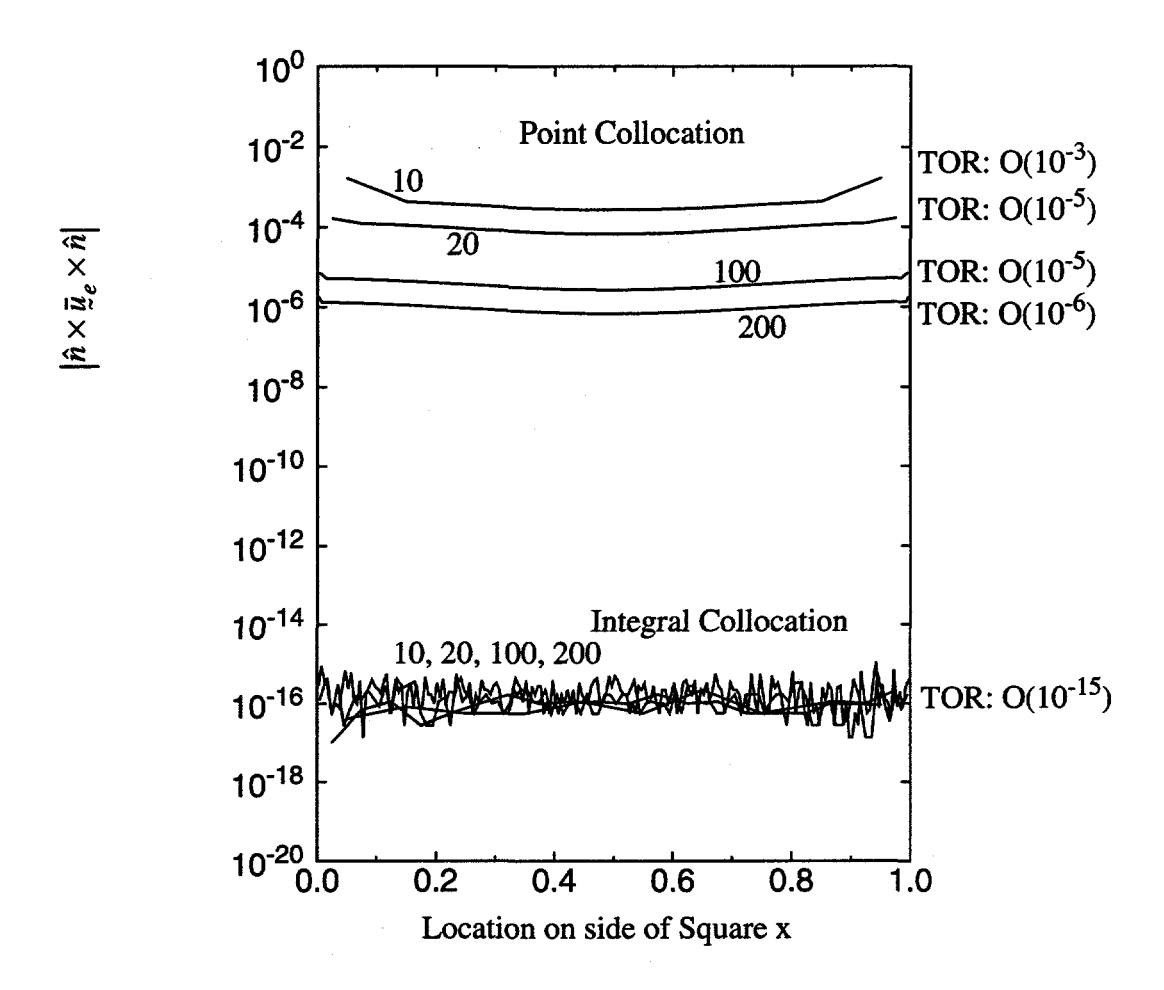


Figure 4 Errors in the tangential velocity boundary condition using point collocation for the point vortex problem. Results are shown for 10, 20, 100, and 200 linear boundary elements per side of the unit square. The residual for the theorem of the rotational (TOR) is also shown.

2. Accuracy Assessment

Two test problems are considered. Results from the proposed method are compared with results from point collocation techniques. The comparison is made for both piece-wise constant boundary elements, and piece-wise linear boundary elements. The domain for both test problems is the interior of the unit square. Many previous investigations indicate that additional integral constraints are needed only in only exterior problems to eliminate the arbitrariness associated with multiply-connected (exterior) domains. As will be shown, even in interior domains, satisfaction of the theorem of the rotational provides a better numerical solution.

The two problems considered are a point vortex centered in the unit square, and a uniform field of unit vorticity in the unit square (Figure 1). The objective in both problems is to solve for the vortex sheets on the boundary that satisfy the zero velocity boundary condi-

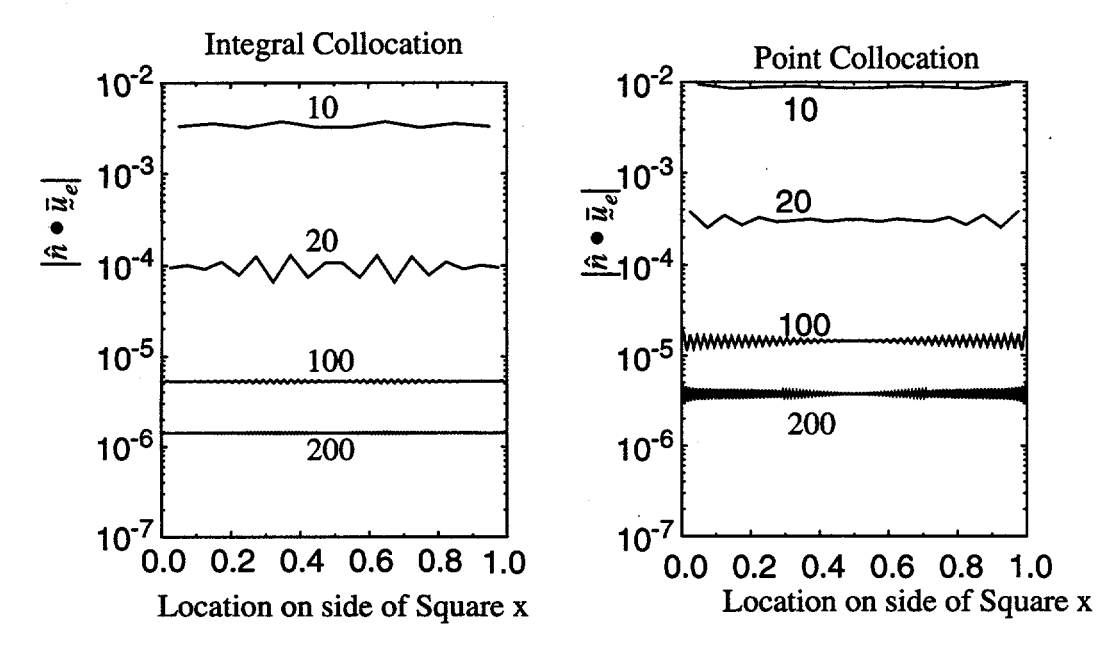


Figure 5 Convergence characteristics for integral collocation and point collocation for the point vortex problem using linear boundary elements. Errors in the normal velocity on the boundary are shown for 10, 20, 100, and 200 boundary elements per side of the unit square.

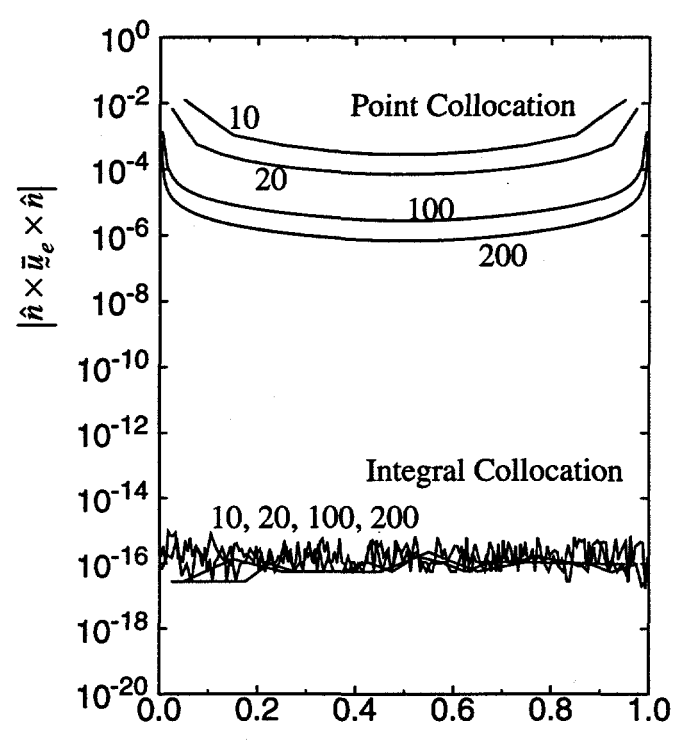
tion. The accuracy of the solutions are assessed by examining the values of the normal and tangential velocities on the boundary. Recall that, analytically, if the tangential component of the velocity boundary condition is satisfied, then the normal component must also be satisfied. In discrete systems, however, the normal velocity is not satisfied exactly, but errors should decrease with increasing resolution.

The two problems considered here were chosen since they include corners, at which it is anticipated that satisfying both components of the velocity boundary condition will be difficult, and therefore a good test of the proposed formulation. Analytical representations for the integrated velocities on each (flat) element are used in these calculations to avoid quadrature errors and thus provide the most accurate solutions.

Average boundary velocity errors $\bar{u}_{e,i}$ are calculated for boundary element i with arc length Δs_i using the computed vortex sheets strengths. Only averages of the velocity on a boundary element are considered, even for point collocation results. Non-zero values of the integrated velocity component are errors since the velocity boundary condition is zero.

$$\hat{n} \times \bar{\underline{u}}_{e,i} \times \hat{n} + \hat{n} [\hat{n} \bullet \bar{\underline{u}}_{e,i}] = \frac{1}{\Gamma \Delta s_i} \int_{S_i} \left\{ \frac{1}{\pi} [\underline{u}_{\omega} + \underline{u}_{\gamma} + \underline{u}_{u_{\tau}} + \underline{u}_{u_{n}}] + \underline{\gamma}_c \times \hat{n}(\underline{x}_b) \right\} dS \qquad (28)$$

 Γ is the circulation contained in the domain. Normalization by this quantity results in the same errors for all values of the circulation for the point vortex and for the constant value



Location on side of Square x

Figure 6 Errors in the tangential velocity boundary condition using point collocation for the unit vorticity in a box problem. Results are shown for 10, 20, 100, and 200 linear boundary elements per side of the unit square.

of vorticity in the problems discussed below. Values of $\bar{u}_{e,i}$ are plotted at the midpoint of each boundary element. The degree to which the theorem of the rotational is satisfied is also examined. The residual quantity that will be reported is

$$\int_{A} \omega dA - \oint (\hat{n} \times \underline{u}_{\omega} - \underline{\gamma}) ds = \Re.$$
 (29)

The Biot-Savart velocity induced on one side of the unit square for the two problems of interest are shown in Figure 1. The integrated tangential velocities on each side of the square are shown in Figure 2. Note that to obtain similar accuracy in satisfying the theorem of the rotational for the Biot-Savart velocity, a much higher resolution is required for the case of unit vorticity than for a point vortex¹. As a result, it will be seen that for similar discretizations, more accurate results will be obtained for the point vortex problem.

^{1.} As shown in Figure 2, for a particular quadrature, integration of the Biot-Savart velocity on the boundary satisfies the theorem of the rotational more accurately for the point vortex problem than the constant vorticity problem. This is due to the fact that, in the analytical solution for the velocity induced by constant vorticity, there are logarithmic terms which are not integrated as accurately by standard Gaussian quadrature as non-logarithmic integrands, such as for the velocity induced by a point vortex. Special quadratures for logarithmic integrands can be used to obtain more accurate results; e.g., [2], but this would complicate the numerical algorithm considerably. This motivates the use of analytical solutions, instead of quadratures in the solutions to be described.

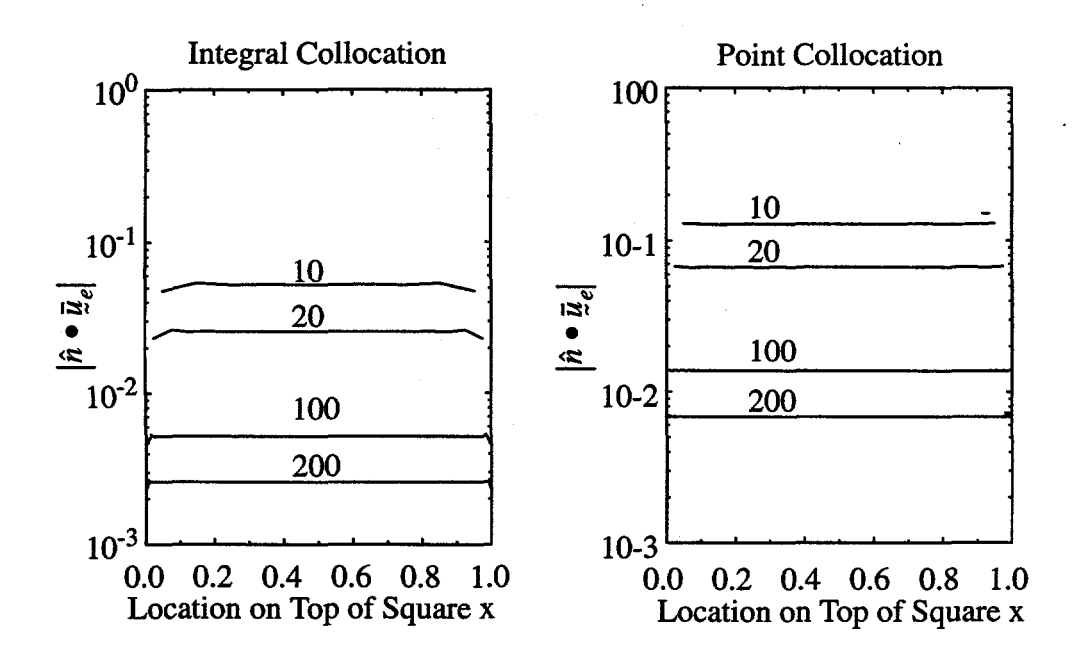


Figure 7 Normal velocity errors on the boundary of the unit square filled with unit vorticity, using 10, 20, 100, and 200 linear boundary elements per side.

Figure 3 shows the boundary velocity errors for the point vortex problem with 20 boundary elements on a side. The different curves are obtained from combinations of point collocation and integral collocation methods, and linear and constant boundary elements. (For the problems of interest, "double noding" for linear elements in the corners is not required due to symmetry.) The best accuracy is for the integral collocation with linear elements. Note that the two integral collocation solutions satisfy the theorem of the rotational and the tangential velocity boundary condition to within 10⁻¹⁵ (for double precision calculations), by design of the integral collocation method. Point collocation methods not only have larger errors in the normal velocity, they also have non-negligible errors in the tangential velocity, and in satisfying the theorem of the rotational. For constant boundary elements, the large errors in the normal velocity at corners decrease very little with increasing resolution. Thus, constant boundary elements are not considered further.

The convergence characteristics for linear boundary elements for the point vortex problem are shown in Figure 4 (tangential velocity errors) and Figure 5 (normal velocity errors). Note that the tangential velocity errors are roughly given by the residual to the theorem of the rotational. The tangential velocity errors for integral collocation are $O(10^{-15})$ for each discretization, which is ten orders of magnitude more accurate than the point collocation results. The residual for the theorem of the rotational is also ten orders of magnitude smaller for the integral collocation method. For errors in the normal velocity, the integral collocation method yields smaller errors for each discretization.

Note that the errors in tangential velocity on the boundary $(O(10^{-15}))$ in Figure 4) are much smaller than the errors in the normal velocity on the boundary (> $O(10^{-6})$) in Figure 5). The much higher accuracy in the tangential velocities might seem unnecessary, but it is not. If

the tangential velocities are not accurate, then the theorem of the rotational is not satisfied accurately. The result of small errors in satisfying the theorem of the rotational can be that errors occur in the vorticity field, and grow with each time step. For example, tangential velocity errors of $O(10^{-2})$ in satisfying the theorem of the rotational can lead to errors of $O(10^{1})$ after a few tens of time steps.

To see why the errors grow with each time step, consider that errors in satisfying the theorem of the rotational generally result in vortex sheet strengths that are too large. After the sheets enter the domain, they induce velocities on the boundary that are too large. In the next time step, the new vortex sheets generated to eliminate the too-large boundary velocities also fail to satisfy the theorem of the rotational. As a result, the new vortex sheet strengths are too large for the too-large velocities on the boundary. In this way, errors in vortex sheet strengths are amplified each time-step, and accumulate rapidly. This is the reason that many formulations explicitly impose an integral constraint on vorticity generation even though it over-specifies the system: failure to accurately satisfy the integral constraint yields large errors in vorticity generation.

Figure 6 shows the convergence properties for tangential velocity errors for point collocation on the unit square filled with unit vorticity, using linear boundary elements. Note that for point collocation, relatively large errors in tangential velocity persist near the corners even for the largest number of boundary elements. Again, the residual to the theorem of the rotational is a rough indication of the tangential velocity errors. Figure 7 shows the convergence properties for errors in the normal velocity. Results for point collocation and integral collocation compare in the same way as before: integral collocation yields better accuracy in satisfying both components of the velocity on the boundary.

Summary

A well-posed method to calculate vortex sheet strengths to satisfy velocity boundary conditions has been formulated and implemented numerically. The main formulation consists of a generalized Helmholtz decomposition (GHD) which depends on the vorticity field, and both components (normal and tangential) of the velocity boundary conditions.

The main conclusion is that a unique, well-posed (*i.e.*, not over-specified) formulation can be obtained by using an integral collocation technique on the tangential component of the GHD. The set of linear equations obtained from the integral collocation method implicitly satisfy the integral constraint on the vortex sheets. Since a well-posed method to determine vortex sheet strengths exists, and since vorticity fluxes can be obtained from vortex sheet strengths, a well-posed, unique vorticity flux can be determined for use in Navier-Stokes simulations.

Discretization errors for the integral collocation method were shown to decrease with decreasing element size faster than point collocation methods, and always provide greater accuracy, particularly in the tangential velocity boundary condition. It was also found that linear boundary elements provide sufficiently greater accuracy than constant elements to warrant the recommendation that constant elements be avoided.

Future activities in this area include using this formulation to solve for nodal vorticity values (rather than vortex sheets) in order to satisfy velocity boundary conditions. This approach would avoid the singular-behavior associated with vortex sheets, and additional boundary velocity errors that occur when the vortex sheets diffuse into the domain.

APPENDIX A Construction of a Generalized Helmholtz Decomposition

A generalized Helmholtz' decomposition is derived. The purpose for this derivation is to make evident the most important features of the generalized Helmholtz' decompositions. These features have not been made clear by previous investigators who used the it (Wu [40], Morino [27], Uhlman [37]). Three important features that have not been sufficiently emphasized previously are:

- 1) Satisfying a single component (normal or tangential) of the generalized Helmholtz' decomposition implies that the other unspecified component is satisfied implicitly. Thus, in principle (that is to say, analytically, but perhaps not numerically) specification of both components of the decomposition on the boundary is an over-specification, and is not necessary. This result is due principally to the fact that the velocity outside the fluid domain is required to be zero.
- 2) The generalized Helmholtz' decomposition implicitly satisfies integral constraints on vorticity field and velocity boundary conditions. As a result, integral constraints (which over-specify the problem and result in errors) should not be necessary (as long as numerical methods implicitly approximate the integral constraint).
- 3) The generalized Helmholtz' decomposition can be used to solve for the vorticity field, rather than vortex sheets, thus avoiding the errors in satisfying velocity boundary conditions that are intrinsic with vortex sheets.¹

An important aspect of the generalized Helmholtz' decomposition is that it essentially addresses the infinite domain, restricting non-zero velocity fields to the fluid domain, and zero velocity outside the fluid. Feature number 1 listed above follows directly from this. Due its importance, extensive discussion is given regarding the zero velocity outside the fluid.

The generalized Helmholtz decomposition is generalized in the sense that the classical Helmholtz decomposition does not contain the velocity boundary conditions, whereas the generalized formulation does, thus making it more general. The classical Helmholtz decomposition specifies a velocity field \underline{u} in terms of a vorticity field $\underline{\omega} = \nabla \times \underline{u}$, and a divergence of the velocity field $D(\underline{x}) = \nabla \bullet \underline{u}$ as (Batchelor [3], Morino [28])

$$\underline{u}(\underline{x}) = \nabla \times \int_{R_m} \underline{\omega}(\underline{x}') G(\underline{x}, \underline{x}') dR(\underline{x}') - \nabla \int_{R_m} D(\underline{x}') G(\underline{x}, \underline{x}') dR(\underline{x}')$$
 A.30

^{1.} The motion induced by zero thickness vortex sheets is much different from the motion induced after a vortex sheet attains a finite thickness due to viscous diffusion. As a result, boundary conditions that are well-satisfied by vortex sheets, are not well-satisfied after the sheets diffuse.

The vorticity and velocity divergence field are integrated over the infinite domain R_{∞} . Points in the domain are denoted by x, and variables of integration are denoted by primes. G(x, x') is the infinite domain Green's function for a Poisson equation. In two-dimensions,

$$G(\underline{x},\underline{x}') = \frac{1}{2\pi} \log \left[\frac{1}{|\underline{x}-\underline{x}'|} \right]$$
 and for three-dimensions, $G(\underline{x},\underline{x}') = \frac{1}{4\pi} \frac{1}{|\underline{x}-\underline{x}'|}$.

The velocity field in Eq. A.30 field is arbitrary to within an incompressible, irrotational velocity field, classically denoted as $\nabla \phi$ (which is irrotational since $\nabla \times \nabla \phi \equiv 0$), where ϕ is a scalar potential that satisfies $\nabla^2 \phi = 0$ (which is obtained by requiring that $\nabla \phi$ is solenoidal, $\nabla \cdot \nabla \phi = 0$). Solutions to Laplace equations admit normal velocity boundary conditions, but do not admit tangential velocity boundary conditions. $\nabla \phi$ is typically added to Eq. A.30 to satisfy the normal velocity boundary condition, but usually does not satisfy the tangential velocity boundary condition. The deviation from the desired tangential velocity boundary condition is treated as a vortex sheet.

The generalized Helmholtz' decomposition allows the tangential velocity boundary condition $\hat{n} \times \underline{u} \times \hat{n}$ to be specified, in addition to the normal velocity boundary condition, $\hat{n} \cdot \underline{u}$. (\hat{n} is the outward pointing unit normal vector on the boundary.)

$$c(\underline{x})\underline{u}(\underline{x}) =$$

$$\nabla \times \int_{R} \underline{\omega}(\underline{x}') G(\underline{x}, \underline{x}') dR(\underline{x}') + \nabla \times \int_{S} [-\hat{n}(\underline{x}_{b}') \times \underline{u}(\underline{x}_{b}')] G(\underline{x}, \underline{x}_{b}') dS(\underline{x}_{b}')$$

$$- \nabla \int_{R} D(\underline{x}') G(\underline{x}, \underline{x}') dR(\underline{x}') - \nabla \int_{S} [-\hat{n}(\underline{x}_{b}') \bullet \underline{u}(\underline{x}_{b}')] G(\underline{x}, \underline{x}_{b}') dS(\underline{x}_{b}')$$

$$+ \nabla \int_{R} D(\underline{x}') G(\underline{x}, \underline{x}') dR(\underline{x}') - \nabla \int_{S} [-\hat{n}(\underline{x}_{b}') \bullet \underline{u}(\underline{x}_{b}')] G(\underline{x}, \underline{x}_{b}') dS(\underline{x}_{b}')$$

The vorticity and velocity divergence field are integrated over the finite or infinite domain R, and the velocity boundary conditions are integrated over S, the surface of the domain. Points on the boundary are denoted by \underline{x}_h . The coefficient c is given by

$$c(\underline{x}) = \begin{cases} 1 \text{ in the domain R} \\ a \text{ on the boundary S} \\ 0 \text{ outside the region R and boundary S} \end{cases}$$
 A.32

 α is the value of the internal angle, divided by 2π for two-dimensional flows, and the internal solid angle divided by 4π in three-dimensional flows. For example, on a smooth boundary of a two-dimensional domain, the internal angle is π , so $\alpha = 1/2$.

In Appendix B, it is shown that for incompressible (D=0), irrotational $(\omega=0)$ flows, the boundary integrals in the generalized Helmholtz' decomposition are analytically equivalent to the potential velocity field $\nabla \phi$ obtained from the solution of $\nabla^2 \phi = 0$. A derivation of the generalized Helmholtz' decomposition is described below.

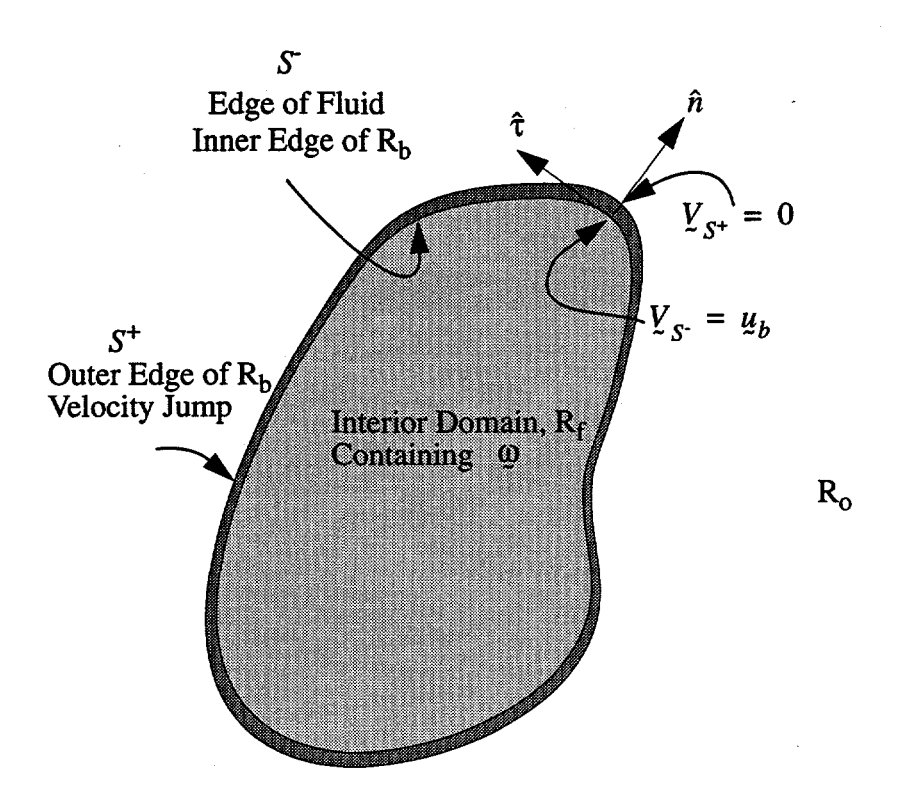


Figure 8 Configuration of fluid and boundary domains, R_f and R_b . The unit normal vector \hat{n} points outward from the fluid. The side of R_b adjacent to the fluid is denoted as S^- , and the other side of R_b is denoted as S^+ .

2. Derivation of the Generalized Helmholtz Decomposition

Derivation of the generalized Helmholtz' decomposition begins by decomposing each of the integrals over the infinite domain into integrals over the fluid domain R_f , a thin region on the boundary of the fluid R_b , and the remainder of the infinite domain R_o , as shown in Figure 8,

$$\int_{R_{\infty}} ()dR = \int_{R_f} ()dR + \int_{R_h} ()dR + \int_{R_g} ()dR$$
 A.33

The vorticity and velocity divergence are specified to be zero in R_o , to prevent the non-physical situation of phenomena outside the fluid influencing fluid. In R_b , the vorticity and velocity divergence are assumed to be non-zero, and although R_b lies outside the fluid, a limiting process will be applied to it so its thickness approaches zero. The zero thickness form of R_b becomes the boundary of the fluid. The vorticity and velocity divergence in R_b

will be affected by the limiting process, and will contribute velocities that are integrably singular on the boundary.

Consider R_b to be defined by a thickness Δn and a surface area dS,

$$dR_b = dS \bullet \Delta n. A.34$$

In the limit as $\Delta \underline{n}$ approaches zero, the boundary region R_b collapses to form the boundary. The limiting process also takes into account the non-zero vorticity and velocity divergence, $\omega \neq 0$ and $D \neq 0$ in R_b . The two surfaces of R_b in Figure 8 are denoted S^+ and S^- . This notation is based on an the definition of a normal unit vector which points outward from the fluid. Accordingly, S^+ is the surface that lies in the positive "+" normal direction from R_b . Similarly, S^- denotes the surface that lies in the negative "-" normal direction from R_b .

2.1 Vortex Sheets

For non-zero vorticity $\underline{\omega}_b$ in the boundary region R_b , consider holding the quantity $\underline{\omega}_b \Delta n$ constant as the thickness is reduced to zero, and $\underline{\omega}_b$ approaches infinity,

$$\gamma = \lim_{\substack{\omega_b \to \infty \\ \Delta n \to 0}} \omega_{\varepsilon} \Delta n \qquad A.35$$

$$\Delta n \to 0 \qquad 0$$

where γ is the strength of a vortex sheet. Note that the normal component of vorticity is zero to satisfy the constraint that vortex lines cannot cross the boundary.

Applying this limiting procedure to the velocity due to ω_b in R_b yields the velocity induced by a vortex sheet on the boundary of the fluid,

$$\lim_{\begin{subarray}{c} \ensuremath{\omega}_{\varepsilon} \to \infty \\ \Delta n \to 0 \\ \hat{n} \bullet \ensuremath{\omega} \to 0 \ensuremath{\rangle}$$

$$A.36$$

$$A.36$$

Note that the specification $\hat{n} \bullet \omega \to 0$ satisfies $\nabla \times \underline{u} = \omega$ since it can be shown that (see Batchelor [3], p. 86)

$$\nabla \times \underline{u} = \underline{\omega} + \int_{S} (\hat{n} \bullet \underline{\omega}) G dS.$$

2.2 Source Sheets

Now consider a region of non-zero velocity divergence D_b in the boundary region R_b . Following a similar procedure as above, a surface distribution of a source σ is defined as

$$\sigma = \lim_{\substack{D_b \to \infty \\ \Delta n \to 0}} D_{\varepsilon} \Delta n.$$
 A.37

Applying this limiting procedure to the velocity due to D_b in R_b yields the velocity induced by a source sheet on the boundary of the fluid,

$$\lim_{\substack{D_b \to \infty \\ \Lambda_B \to 0}} \nabla \int_R D_b(\underline{x}') G(\underline{x}, \underline{x}') dR(\underline{x}') \to \nabla \int_S \sigma(\underline{x}'_b) G(\underline{x}, \underline{x}') dS(\underline{x}_b') \quad . \tag{A.38}$$

Applying these new boundary integrals to the domain decomposition Eq. A.33 yields,

$$\underline{u}(\underline{x}) = A.39$$

$$\nabla \times \int_{R} \omega(\underline{x}') G(\underline{x}, \underline{x}') dR(\underline{x}') + \nabla \times \int_{S} \underline{\gamma}(\underline{x}_{b}') G(\underline{x}, \underline{x}_{b}') dS(\underline{x}_{b}')$$

$$-\nabla \int_{R} D(\underline{x}')G(\underline{x},\underline{x}')dR(\underline{x}') - \nabla \int_{S} \sigma(\underline{x}'_{b})G(\underline{x},\underline{x}_{b}')dS(\underline{x}_{b}')$$

The boundary integrals in Eq. A.36 and Eq. A.38 are integrably singular at points x_b on the boundary (Kellog [14]). At a boundary point where the internal angle of the boundary is β , (and d = 2 denotes two-dimensional region, d = 3 denotes a three-dimensional region, and $\alpha = +1$ on S^+ and $\alpha = -1$ on S^-), the boundary integral containing the vortex sheet strength has the value

$$\nabla \times \int_{S} \underline{\gamma}(\underline{x}_{b}') G(\underline{x}, \underline{x}'_{b}) dS(\underline{x}_{b}') =$$

$$-\frac{\alpha \beta}{2\pi (d-1)} \hat{n}(\underline{x}_{b}) \times \underline{\gamma}(\underline{x}_{b})] + \nabla \times \int_{S(\underline{x}'_{b} \neq x_{b})} \underline{\gamma}(\underline{x}_{b}') G(\underline{x}, \underline{x}'_{b}) dS(\underline{x}_{b}')$$

$$A.40$$

Similarly, on the boundary, the boundary integral containing the source sheet strength has the value

$$\nabla \int_{S} \sigma(\underline{x}') G(\underline{x}, \underline{x}') dS(\underline{x}_{b}') = \frac{\alpha \beta}{2\pi (d-1)} \hat{n}(\underline{x}_{b}) \sigma(\underline{x}_{b}) + \nabla \int_{S(\underline{x}_{b}' \neq x_{b})} \sigma(\underline{x}, \underline{x}') dS(\underline{x}_{b}') \text{ A.41}$$

These results indicate that there is a velocity jump across the boundary. To show this, denote u_1 as the non-singular contribution to the velocity at a point on the boundary,

$$\begin{split} & \underline{u}_1 = \nabla \times \int_{\underline{\omega}} \underline{\omega}(\underline{x}') G(\underline{x},\underline{x}') dR(\underline{x}') - \nabla \int_{\underline{\omega}} D(\underline{x}') G(\underline{x},\underline{x}') dR(\underline{x}') \\ & \nabla \times \int_{\underline{S}(\underline{x}'_b \neq x_b)} \underline{\gamma}(\underline{x}'_b) G(\underline{x},\underline{x}'_b) dS(\underline{x}_b') - \nabla \int_{\underline{S}(\underline{x}'_b \neq x_b)} \underline{\sigma}(\underline{x}_b') G(\underline{x},\underline{x}') dS(\underline{x}_b') \end{split}$$

The restriction $\underline{x}_b \neq \underline{x}_b'$ on the limits of the boundary integrals indicates that $\underline{u}_1(\underline{x}_b)$ has the same value at $S^+(\underline{x}_b)$ and $S^-(\underline{x}_b)$. The velocity jump at \underline{x}_b is due to $\underline{\gamma}(\underline{x}_b)$ and $\sigma(\underline{x}_b)$, and is not included in $\underline{u}_1(\underline{x}_b)$.

The velocity on S^+ is

$$\underline{u}_{S^{+}} = \frac{-\beta}{2\pi(d-1)}(\hat{n}(\underline{x}_{b}) \times \underline{\gamma}(\underline{x}_{b})) + \frac{\beta}{2\pi(d-1)}\hat{n}(\underline{x}_{b})\sigma(\underline{x}_{b}) + \underline{u}_{1} \quad , \qquad A.42$$

and the velocity on S

$$\underline{u}_{S} = \frac{\beta}{2\pi(d-1)}(\hat{n}(\underline{x}_b) \times \underline{\gamma}(\underline{x}_b)) - \frac{\beta}{2\pi(d-1)}\hat{n}(\underline{x}_b)\sigma(\underline{x}_b) + \underline{u}_1 \quad . \tag{A.43}$$

Subtracting these equations yields the tangential and normal velocity jumps across the boundary

$$\underline{u}_{S^+} - \underline{u}_{S^-} = \frac{-\beta}{\pi(d-1)} (\hat{n}(\underline{x}_b) \times \underline{\gamma}(\underline{x}_b)) + \frac{\beta}{\pi(d-1)} \hat{n}(\underline{x}_b) \sigma(\underline{x}_b) \quad . \tag{A.44}$$

Values for the vortex sheet and source sheet strengths can be specified in terms of $u_{S^+} - u_{S^-}$ as

$$\gamma(x_b) = \frac{\beta}{2\pi(d-1)} \hat{n}(x_b) \times [u_{S^+}(x_b) - u_{S^-}(x_b)]$$
A.45

(using $\hat{n}(\underline{x}_b) \times [-\hat{n}(\underline{x}_b) \times \underline{\gamma}(\underline{x}_b)] = \underline{\gamma}(\underline{x}_b)$ since $\underline{\gamma}$ has components only in the tangential directions, according to the definition Eq. A.35) and

$$\sigma(\underline{x}_b) = \frac{\beta}{2\pi(d-1)}\hat{n}(\underline{x}_b) \bullet [\underline{u}_{S^+}(\underline{x}_b) - \underline{u}_{S^-}(\underline{x}_b)] \quad . \tag{A.46}$$

On smooth boundaries, $\beta/(\pi(d-1)) = 1$, which is the case we consider hereafter.

Substituting
$$\underline{\gamma}(\underline{x}_b) = \hat{n}(\underline{x}_b) \times [\underline{u}_{S^+}(\underline{x}_b) - \underline{u}_{S^-}(\underline{x}_b)]$$
 and $\sigma(\underline{x}_b) = \hat{n}(\underline{x}_b) \bullet [\underline{u}_{S^+} - \underline{u}_{S^-}]$

into the Helmholtz decomposition evaluated on S^+ (Eq. A.42) yields (for $\beta/(\pi d) = 1$)

$$\underline{u}_{S^+} = \underline{u}_1 +$$
 A.47

$$\frac{1}{2}[\hat{n}(\underline{x}_b)\times[\underline{u}_{S^+}(\underline{x}_b)-\underline{u}_{S^-}(\underline{x}_b)]\times\hat{n}(\underline{x}_b)+\hat{n}(\underline{x}_b)\{\hat{n}(\underline{x}_b)\bullet[\underline{u}_{S^+}(\underline{x}_b)-\underline{u}_{S^-}(\underline{x}_b)]\}]$$

and on S^- (Eq. A.43)

$$\begin{split} \underline{u}_{S^-} &= \underline{u}_1 - \\ &\frac{1}{2} [\hat{n}(\underline{x}_b) \times [\underline{u}_{S^+}(\underline{x}_b) - \underline{u}_{S^-}(\underline{x}_b)] \times \hat{n}(\underline{x}_b) + \hat{n}(\underline{x}_b) \{\hat{n}(\underline{x}_b) \bullet [\underline{u}_{S^+}(\underline{x}_b) - \underline{u}_{S^-}(\underline{x}_b)]\}] \end{split}$$

Representing u_{S^+} and u_{S^-} on the left-hand side of the two above equations in normal and tangential components

$$\underline{u}_i = \hat{n} \times \underline{u}_i \times \hat{n} + \hat{n}(\hat{n} \bullet \underline{u}_i)$$

The equations for u_{S^+} and u_{S^-} become identical (dropping the notation $\hat{n}(x_b)$)

$$\frac{1}{2}[\hat{n} \times [\underline{u}_{S^{+}} + \underline{u}_{S^{-}}] \times \hat{n} + \hat{n}(\hat{n}[\underline{u}_{S^{+}} + \underline{u}_{S^{-}}])] = \underline{u}_{1}$$
 A.48

or, simply,

$$\frac{1}{2}(u_{S^+} + u_{S^-}) = u_1 \tag{A.49}$$

so that "evaluation on the boundary" has a unique meaning, even though there is a velocity jump across the boundary.

2.3 Assignment of Values for u_{S^+} and u_{S^-}

Next, the generalized Helmholtz decomposition is completed by assigning values for u_{S^+} and u_{S^-} . We assign the velocity boundary condition for the fluid to be u_{S^-} , since u_{S^-} is the velocity on the fluid side of the boundary.

On the other side of the boundary lies the boundary of the non-fluid region which contains zero vorticity and zero velocity divergence. Accordingly, $u_{S^+} = \nabla \phi_{S^+}$, with $\nabla^2 \phi = 0$, and, at infinity, $\nabla \phi = 0$, where the location of this boundary condition is assumed to extend beyond the location associated with any velocity boundary condition at infinity (e.g., see Batchelor, p 86). Thus, $u_{S^+} = \nabla \phi$ must satisfy the constraints

$$\int_{S^{+}} \nabla \phi \bullet \hat{n} \ dS = 0 \text{ and } \int_{S^{+}} \nabla \phi \bullet \hat{\tau} dS = 0.$$
 A.50

We note that there are an infinite number of choices that will satisfy these constraints, and for each different domain of interest, we could specify any one of the infinite choices for

the von Neumann boundary condition $\hat{n} \cdot \nabla \phi_{S^+}$ and solve $\nabla^2 \phi = 0$ (in the region outside the fluid) to determine $\hat{\tau} \cdot \nabla \phi_{S^+}$, to fully define the velocity $\nabla \phi_{S^+}$. Such a procedure would be inconvenient to say the least, but having defined $u_{S^+} = \nabla \phi_{S^+}$, the generalized Helmholtz decomposition would be complete.

One particular choice, however, is very convenient, and also allows the specification of a Dirichlet condition in addition to the von Neumann condition, thus making it very general. The choice of interest is $u_{S^+} = 0$, which clearly satisfies both integral constraints on the velocity boundary condition.

First, consider the von Neumann condition, $\nabla \phi \bullet \hat{n} = 0$. The solution for this boundary condition is well-known to be $\nabla \phi = 0$ everywhere, including on S^+ , $\nabla \phi \bullet \hat{\tau} = 0$ on S^+ , which is consistent with $u_{S^+} = 0$. (Batchelor [3])

Next, consider the boundary condition $\nabla \phi \bullet \hat{\tau} = 0$ on S^+ . $\nabla \phi \bullet \hat{\tau} = 0$ implies that $\phi =$ constant on the boundary. Then, from the maximum-minimum modulus theorem (which states that harmonic functions can have maxima and minima only on boundaries²), if the velocity is zero on S^+ , and zero at infinity, then $\nabla \phi = 0$ everywhere outside the fluid, including $\nabla \phi \bullet \hat{n} = 0$ on S^+ .

Thus, the choice of $u_{S^+} = 0$ provides a valid and convenient choice, and yields the final result,

$$c(\underline{x})\underline{u}(\underline{x}) =$$

$$\nabla \times \int_{R} \underline{\omega}(\underline{x}')G(\underline{x},\underline{x}')dR(\underline{x}') + \nabla \times \int_{S} [-\hat{n}(\underline{x}_{b}') \times \underline{u}(\underline{x}_{b}')]G(\underline{x},\underline{x}_{b}')dS(\underline{x}_{b}')$$

$$-\nabla \int_{R} D(\underline{x}')G(\underline{x},\underline{x}')dR(\underline{x}') - \nabla \int_{S} [-\hat{n}(\underline{x}_{b}') \bullet \underline{u}(\underline{x}_{b}')]G(\underline{x},\underline{x}_{b}')dS(\underline{x}_{b}')$$

$$A.52$$

To examine the meaning of the boundary integrals, define the linear operator

^{2.} The maximum-minimum modulus theorem applies to closed bounded regions; *i.e.*, the theorem is not generally stated as applying to unbounded domains. However, as described by Wu [39] and Morino [27], velocity boundary conditions at infinity can be properly represented by the boundary integrals in Eq. A.39 when the integrals are applied to a boundary whose location approaches infinity. In this sense, all domains can be considered as bounded.

$$L(\underline{u}) = \nabla \times \int_{S} [-\hat{n}(\underline{x}_{b}') \times \underline{u}(\underline{x}_{b}')] G(\underline{x}, \underline{x}_{b}') dS(\underline{x}_{b}') -$$

$$\nabla \int_{S} [-\hat{n}(\underline{x}_{b}') \bullet \underline{u}(\underline{x}_{b}')] G(\underline{x}, \underline{x}_{b}') dS(\underline{x}_{b}')$$
A.53

Substitute the classical decomposition for incompressible flows,

$$\underline{u} = \underline{u}_{\omega} + \nabla \Phi$$
 A.54

where

$$\underline{u}_{\omega} = \nabla \times \int_{R} \underline{\omega}(\underline{x}') G(\underline{x}, \underline{x}') dR(\underline{x}') . \qquad A.55$$

Eq. A.51 becomes

$$c(x)u(x) = u_{\omega} + L(u_{\omega}) + L(\nabla \phi)$$
 A.56

The terms $\underline{u}_{\omega} + L(\underline{u}_{\omega})$ equals \underline{u}_{ω} in the domain, and zero outside the domain. ($L(\underline{u}_{\omega})$ is zero in the domain, and $-\underline{u}_{\omega}$ outside the domain.)

The term $L(\nabla \phi)$ is shown in Appendix B to be the solution to $\nabla^2 \phi = 0$, which allows tangential velocity boundary conditions to be calculated directly, without having to first find ϕ and then differentiate it.

APPENDIX B: Validation of a Generalized Potential Velocity Field

Overview

A formulation is derived for incompressible, irrotational flows that allows tangential or normal velocity boundary conditions to be specified. In contrast, the classical potential formulation for incompressible, irrotational flows does not allow the tangential velocity boundary condition to be specified. The opportunity to specify the tangential velocity boundary condition has application in three areas:

- 1. creation of continuous vorticity (not vortex sheets) to satisfy velocity boundary conditions,
- 2. simplification of non-uniqueness issues in multiply-connected domains, and
- 3. methodology to calculate velocities on "outflow" boundaries without the use of *ad hoc* assumptions.

The formulation which admits the tangential velocity boundary condition is shown to be equivalent to the classical formulation for potential velocity fields.

Introduction

Velocity fields \underline{u} which are incompressible $\nabla \bullet \underline{u} = 0$ and irrotational $\nabla \times \underline{u} = 0$ are classically described as the gradient of a velocity potential $\nabla \phi$ (since $\nabla \times \phi \equiv 0$), in which the velocity potential ϕ satisfies the Laplace equation,

$$\nabla^2 \Phi = 0.$$
 B.1

(obtained from requiring $\nabla \bullet \underline{u} = \nabla \bullet \nabla \phi = 0$).

A generalization of Helmholtz' decomposition includes two surface integrals which yield a potential (incompressible and irrotational) velocity field. This formulation allows a potential velocity field to be determined using tangential velocity boundary conditions. This type of boundary condition is not admitted in the classical approach to determine potential velocity fields, which is based on a Laplace equation for the velocity potential. Thus, the generalized Helmholtz' formulation has a distinct advantage over classical formulations.

The objective of this appendix is to show analytically the equivalence of the potential velocity portion of the generalized Helmholtz decomposition and the classical potential velocity field obtained from solving Laplace's equation.

With Dirichlet ϕ and/or von Neumann $\hat{n} \bullet \nabla \phi$ boundary conditions, Eq. B.1 can be solved for ϕ , and then differentiated to obtain the velocity field $\nabla \phi$. It is shown that the velocity field due to the surface integrals in the generalized decomposition is equal to $\nabla \phi$.

To compare the classical and Helmholtz formulations, the boundary element solution to Eq. B.1 is considered

$$\phi(\underline{x}) = -\int_{S} \phi(\underline{x}') \frac{\partial G(\underline{x}, \underline{x}')}{\partial n(\underline{x}')} dS(\underline{x}') + \int_{S} \frac{\partial \phi(\underline{x}')}{\partial n(\underline{x}')} G(\underline{x}, \underline{x}') dS$$
B.2

where Dirichlet and von Neumann boundary conditions can be specified in the integrals over the surface S. Spatial points are denoted as \underline{x} , and integration variables are denoted with a prime. $G(\underline{x},\underline{x}')$ is the *infinite* domain Green's function. \hat{n} is the outward pointing unit normal vector on the surface. Once ϕ is determined from Eq. B.2, the potential velocity field can be obtained by evaluating,

$$\nabla \phi(\underline{x}) = -\nabla \int_{S} \phi(\underline{x}') \frac{\partial G(\underline{x}, \underline{x}')}{\partial n(\underline{x}')} dS(\underline{x}') + \nabla \int_{S} \frac{\partial \phi(\underline{x}')}{\partial n(\underline{x}')} G(\underline{x}, \underline{x}') dS \quad . \tag{B.3}$$

The generalized Helmholtz' decomposition is

$$c(\underline{x})\underline{u}(\underline{x}) = B.4$$

$$\nabla \times \int_{R} \underline{\omega}(\underline{x}') G(\underline{x}, \underline{x}') dR(\underline{x}') + \nabla \times \int_{S} [-\hat{n}(\underline{x}_{b}') \times \underline{u}_{b}(\underline{x}_{b}')] G(\underline{x}, \underline{x}_{b}') dS(\underline{x}_{b}')$$

$$-\nabla \int_{R} D(\underline{x}')G(\underline{x},\underline{x}')dR(\underline{x}') - \nabla \int_{S} (-[\hat{n}(\underline{x}_{b}') \bullet \underline{u}_{b}(\underline{x}_{b}')])G(\underline{x},\underline{x}_{b}')dS(\underline{x}_{b}')$$

In this formulation, $\underline{\omega} = \nabla \times \underline{u}$ is the vorticity, $D = \nabla \bullet \underline{u}$ is the expansion rate of the fluid, and \underline{u}_b is the velocity boundary condition. In the domain, c = 1 on smooth boundaries c = 1/2, and on non-smooth boundaries, c is representative of an interior angle. The surface integrals represent an additive incompressible, irrotational flow which must satisfy the constraint on tangential velocity

$$\int_{\mathbb{R}^{-}} \omega dR = \int_{S} \hat{n} \times \underline{u}_{b} dS.$$
 B.5

The classical formulation must satisfy the more limited case,

$$\int_{S} \hat{n} \times \underline{u}_b dS = 0$$
 B.6

We focus on the incompressible, irrotational velocity field from the generalized decomposition $(\omega = D = 0)$

$$\underline{u}(\underline{x}) = \nabla \times \int_{S} [-\hat{n}(\underline{x}') \times \underline{u}_{b}(\underline{x}')] G(\underline{x}, \underline{x}') dS(\underline{x}') - \nabla \int_{S} (-[\hat{n}(\underline{x}') \bullet \underline{u}_{b}(\underline{x}')]) G(\underline{x}, \underline{x}_{b}') dS(\underline{x}')$$

Note that the tangential velocity on the boundary appears in the first integral in Eq. B.4. This formulation is not well-known, hence we are motivated to show that it is equivalent to the classical potential formulation.

Equivalence of Generalized and Classical Formulations for Incompressible, Irrotational Flows

To begin the comparison of the two formulations, note that $\partial \phi / \partial n$ in Eq. B.3 and $\hat{n} \bullet \underline{u}_b$ in Eq. B.4 are the normal velocity boundary condition. For $\partial \phi / \partial n = \hat{n} \bullet \underline{u}_b$, the two integrals containing these terms are exactly the same. Thus, it remains to be shown that

$$\nabla \times \int_{S} [-\hat{n}(\underline{x}') \times \underline{u}_{b}(\underline{x}')] G(\underline{x}, \underline{x}') dS(\underline{x}') = -\nabla \int_{S} \phi(\underline{x}') \frac{\partial G(\underline{x}, \underline{x}')}{\partial n(\underline{x}')} dS(\underline{x}') \qquad . \tag{B.7}$$

In fact, this equation is derived in Morino'93, with the exception of a contour integral which is zero for a closed surface, such as the surface encompassing a fluid domain. (Morino entitled the proof as "Equivalence of Doublet and Vortex Layers.") In Morino'85 [27], Eq. B.7 is described as "well-known," citing Batchelor [3] (exercise 4 in chapter 3) and Campbell [6], p. 258-260. But, in Morino'93 [28], it is noted that the only *published* proof is given in an Army research report coauthored by Morino, who describes the proof as "cumbersome." The proof discussed here is from Morino'93 [28] with a few (excruciating?) details added for clarity.

Morino's ('93) [28] proof is "given for a flat surface (on which the normal is constant) since the proof for a general smooth surface S can be obtained by approximating a surface with the union of small triangular flat elements and taking the limit as the element dimensions vanish, in which the contributions of the contour integrals (that will be seen to arise) cancel out except for the outer contour."

The basic approach described below is to manipulate the left hand side of Eq. B.7 until it matches the right-hand side.

To begin, recognize that

$$-\hat{n} \times \underline{u}_b = -\hat{n} \times \nabla_S \Phi, \qquad B.8$$

where ∇_{S} is the surface gradient operator defined by 1

$$\nabla_{S}(\) = -\hat{n} \times \hat{n} \times \nabla(\) \text{ or } \nabla_{S}(\) = \hat{\tau} \frac{\partial(\)}{\partial \tau}$$
 B.9

^{1.} The surface gradient operator is needed as a result of the fact that ϕ is a doublet strength. That is, since ϕ is the coefficient of $\partial G/\partial n$ in a surface integral, $\phi(\underline{x})$ represents a jump in ϕ at \underline{x} from a value of $\phi(\underline{x})$ on the domain-side of the boundary, to a value of $\phi=0$ on the non-domain side of the boundary. The normal derivative of such a jump is not defined, and is excluded accordingly in the definition of ∇_S . Similarly, $-\hat{n} \times \underline{u}_b$ is a vortex sheet strength, which is a jump in tangential velocity across the boundary from $-\hat{n} \times \hat{n} \times \underline{u}_b$ to 0; the vortex sheet strength is $\hat{n} \times (0 - \underline{u}_b)$, or $-\hat{n} \times \underline{u}_b$.

where the operator $-\hat{n} \times \hat{n} \times ($) extracts the tangential component of any vector, and $\hat{\tau}$ is the unit tangent vector.

Now, new notation is introduced. The gradient with respect to variables of integration (denoted with primes) is denoted as

$$\nabla = \frac{\partial}{\partial x'} + \frac{\partial}{\partial y'} + \frac{\partial}{\partial z'},$$
 B.10

and the gradient of non-integration variables is

$$\nabla_* = \frac{\partial}{\partial x} + \frac{\partial}{\partial y} + \frac{\partial}{\partial z}.$$
 B.11

Substituting Eq. B.8 into in Eq. B.7 and then applying the curl operator yields

$$\nabla_* \times \int_S [-\hat{n}(\underline{x}') \times \underline{u}_b(\underline{x}')] G(\underline{x}, \underline{x}') dS(\underline{x}')$$

$$= \nabla_* \times \int_S [-\hat{n}(\underline{x}') \times \nabla_S \phi(\underline{x}')] G(\underline{x}, \underline{x}') dS(\underline{x}')$$

$$= \int_S \nabla_* G(\underline{x}, \underline{x}') \times [-\hat{n}(\underline{x}') \times \nabla_S \phi(\underline{x}')] dS(\underline{x}')$$
B.12

Using the relation $\nabla_* G = -\nabla G$, this equation becomes

$$\nabla_* \times \int_S [-\hat{n}(\underline{x}') \times \underline{u}_b(\underline{x}')] G(\underline{x}, \underline{x}') dS(\underline{x}') = \int_S \nabla G(\underline{x}, \underline{x}') \times [\hat{n}(\underline{x}') \times \nabla_S \phi(\underline{x}')] dS(\underline{x}') \quad . \quad \text{B.13}$$

Now, use the identity $a \times (b \times c) = b(a \cdot c) - c(a \cdot b)$ to obtain (omitting functional dependencies for clarity)

$$\nabla_* \times \int_{S} [-\hat{n} \times \nabla_S \phi] G dS = \int_{S} \hat{n} [\nabla G \bullet \nabla_S \phi] dS(\underline{x}') - \int_{S} \nabla_S \phi [\nabla G \bullet \hat{n}] dS$$
 B.14

The first integral on the right hand side can be re-expressed using

$$\nabla_{S} \bullet (\phi \nabla G) = \nabla G \bullet \nabla_{S} \phi + \phi \nabla_{S} \bullet \nabla G$$
 B.15

and using the surface divergence theorem [38] (assuming the normal unit vector is constant, as described following Eq. B.7)

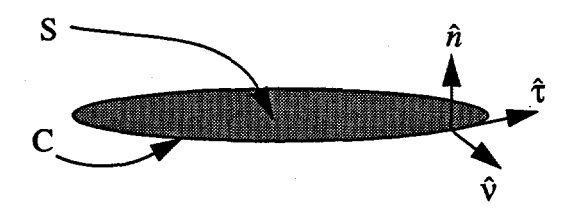


Figure 9. On a planar surface S, the normal unit vector is \hat{n} . The boundary of the surface is C, which has unit normal \hat{v} , and unit tangent $\hat{\tau} = \hat{n} \times \hat{v}$.

$$\int_{S} \nabla_{S} \bullet (\phi \nabla G) dS = \oint_{C} \phi \nabla G \bullet \hat{\mathbf{v}} ds - \int_{S} \kappa \hat{n} \bullet (\phi \nabla G) dS$$
 B.16

where C is the perimeter of the surface S, and ds is the differential arc length of C, and \hat{v} is the outward pointed normal of C, which lies in the plane tangent to S. (See Figure 1.) The curvature is κ (which Morino omitted, but which cancels with a similar integral that was also omitted later in the prooof).

Using equations Eq. B.15 and Eq. B.16, the first integral on the right hand side of Eq. B.14 becomes (again, assuming the normal unit vector is constant)

$$\int_{S} \hat{n} [\nabla G \bullet \nabla_{S} \phi] dS = -\int_{S} \hat{n} \phi (\nabla_{S} \bullet \nabla G) dS + \oint_{C} \hat{n} \phi (\nabla G \bullet \hat{\mathbf{v}}) dS - \int_{S} \hat{n} \kappa (\phi \hat{n} \bullet \nabla G) dS \qquad \text{B.17}$$

The coefficient $\nabla_S \bullet \nabla G$ is represented by noting that (for a unit tangent vector $\hat{\tau}$)

$$\nabla_{S} \bullet \nabla G = \hat{\tau} \frac{\partial}{\partial \tau} \bullet \left(\hat{n} \frac{\partial G}{\partial n} + \hat{\tau} \frac{\partial G}{\partial \tau} \right) = \frac{\partial^{2} G}{\partial \tau^{2}} = \nabla_{S}^{2} G,$$
 B.18

and

$$\nabla^2 G = \nabla_S^2 G + \frac{\partial^2 G}{\partial n^2}.$$
 B.19

A crucial step in Morino's proof is that $\nabla^2 G = 0$ on S for x not on S, so that

$$\nabla_S^2 G = -\frac{\partial^2 G}{\partial n^2},$$
 B.20

Finally, the first integral on the right hand side of Eq. B.14 becomes

$$\int_{S} \hat{n} [\nabla G \bullet \nabla_{S} \phi] dS = \int_{S} \hat{n} \phi \frac{\partial^{2} G}{\partial n^{2}} dS + \oint_{C} \hat{n} \phi (\nabla G \bullet \hat{\mathbf{v}}) ds .$$
 B.21

Now, the second integral on the right hand side of Eq. B.14 can be expressed using

$$\nabla_{S}(\phi \nabla G \bullet \hat{n}) = (\nabla_{S} \phi)(\nabla G \bullet \hat{n}) + \phi \nabla_{S}(\nabla G \bullet \hat{n})$$
B.22

and the surface gradient theorem [38]

$$\int_{S} \nabla_{S} (\phi \nabla G \bullet \hat{n}) dS = \oint_{C} (\phi \nabla G \bullet \hat{n}) \hat{v} ds - \int_{S} \hat{n} \kappa \phi \nabla G \bullet \hat{n} dS .$$
 B.23

(Morino also omitted the curvature term in Eq. B.23.) Using Eq. B.22 and Eq. B.23, the second integral on the right hand side of Eq. B.14 becomes,

$$\int_{S} (\nabla_{S} \phi) (\nabla G \bullet \hat{n}) dS = -\int_{S} \phi \nabla_{S} (\nabla G \bullet \hat{n}) dS + \oint_{C} \phi (\nabla G \bullet \hat{n}) \hat{v} ds - \int_{S} \hat{n} \kappa \phi \nabla G \bullet \hat{n} dS \qquad B.24$$

Using equations Eq. B.21 and Eq. B.24, Eq. B.14 becomes

$$\nabla_{*S} \times \int_{S} [-\hat{n} \times \nabla_{S} \phi] G dS =$$

$$\int_{S} \phi \left[\hat{n} \frac{\partial^{2} G}{\partial n^{2}} + \nabla_{S} \frac{\partial G}{\partial n} \right] dS + \oint_{C} \phi \left[\hat{n} (\nabla G \bullet \hat{v}) - \hat{v} (\nabla G \bullet \hat{n}) \right] dS$$
B.25

Noting that

$$\hat{n}\frac{\partial^2 G}{\partial n^2} + \nabla_S \frac{\partial G}{\partial n} = \left(\hat{n}\frac{\partial}{\partial n} + \nabla_S\right)\frac{\partial G}{\partial n} = \nabla\frac{\partial G}{\partial n}$$
B.26

$$\nabla_* \times \int_S [-\hat{n} \times \nabla_S \phi] G dS = \int_S \phi \left[\nabla \frac{\partial G}{\partial n} \right] dS + \oint_C \phi [\hat{n} (\nabla G \bullet \hat{v}) - \hat{v} (\nabla G \bullet \hat{n})] dS$$
 B.27

In the line integral, once again use the identity $a \times (b \times c) = b(a \cdot c) - c(a \cdot b)$ to re-express the integrand as

$$\nabla_* \times \int_{S} [-\hat{n} \times \nabla_S \phi] G dS = \int_{S} \phi \left[\nabla \frac{\partial G}{\partial n} \right] dS + \oint_{C} \phi \nabla G \times d\underline{s}$$
 B.28

where $ds = \hat{n} \times \hat{v} ds$ is the differential arc length in the tangential direction.

Using $\nabla_* G = -\nabla G$ and $\nabla G \times d\underline{s} = -\nabla_* \times G d\underline{s}$ on the right hand side of the above equation, yields

$$\nabla_* \times \int_{S} [-\hat{n} \times \nabla_S \phi] G dS = -\nabla_* \int_{S} \phi \frac{\partial G}{\partial n} dS - \nabla_* \times \oint_{C} \phi \nabla G \times d\underline{s}$$
 B.29

The contour integral represents the motion associated with a jump in potential within the domain, which we need not include. Thus, for a domain containing no jumps in potential or vortex sheets,

$$\nabla_* \times \int_{S} [-\hat{n} \times \nabla_S \phi] G dS = -\nabla_* \int_{S} \phi \frac{\partial G}{\partial n} dS , \qquad B.30$$

which proves that Eq. B.7 is correct. Thus, the potential velocity field obtained from the generalized decomposition is equal to the classical potential velocity field, and is therefore a valid method to specify potential velocity fields.

References

- Anderson, C. R., "Vorticity Boundary Conditions and Boundary Vorticity Generation for Two-Dimensional Viscous Incompressible Flow," *Journal of Computational Physics*, vol. 80, pp. 72-97, 1989.
- Bannerjee, P.K. and R. Buttterfield, <u>Boundary Element Methods in Engineering and Science</u>, McGraw-Hill Book Company (UK) Limited, 1981.
- Batchelor, G. K., <u>An Introduction to Fluid Mechanics</u>, Cambridge University Press, 1967.
- 4 Brebbia, Telles, Wrobel, Boundary Element Techniques, <u>Theory and Application in Engineering</u>, Springer-Verlag, 1984.
- 5 Bykhovskiy, E. B. and N. V. Smirnov, "On Orthogonal Expansions of the Space of Vector Functions which are Square-Summable over a Given Domain and the Vector Analysis Operators," NASA TM-77051, 1983.
- 6 Campbell, R. G., Foundations of Fluid Flow Theory, Addison-Wesley, 1973.
- 7 Chorin, A. J. and J. E. Marsden, <u>A Mathematical Introduction to Fluid Mechanics</u>, Second Edition, Springer-Verlag, 1990
- Daube. O., "Resolution of the 2D Navier-Stokes Equations in Velocity-Vorticity Form by Means of an Influence Matrix," *Journal of Computational Physics*, vol. 103, pp. 402-414, 1992.
- 9 Gastski, T. B., Grosch, C. E., and M. E. Rose, "the Numerical Solution of the Navier-Stokes Equations for 3-Dimensional, Unsteady, Incompressible Flows by Compact Scheme," J. Fl. Mech., vol. 82, pp. 298-329, 1989.
- 10 Gresho, P. M., "Incompressible Fluid Dynamics: Some Fundamental Formulation Issues," *Ann. Rev. Fluid Mech.*, vol. 23, pp. 413-453, 1991.
- Hess, J. L, "Review of Integral-Equation Techniques for solving Potential Flow Problems with Emphasis on the Surface-Source Method," Comp. Methods in Applied Mech. and Eng., vol. 5, pp. 145-196, 1975.
- Hess, J. L., "Panel Methods in Computational Fluid Dynamics," Ann. Rev. Fluid Mech., vol. 22, 1990.
- Hung, S. C., and R.B. Kinney, "Unsteady Viscous flow over a Grooved Wall: A Comparison of two Numerical Methods, *Int. J. Numer. Methods Fluids*, vol. 8, pp. 1403-1437, 1988.
- 14 Kellog, O. D, Foundations of Potential Theory, Dover, 1953.

- 15 Kempka, S.N., Strickland, J.H., Glass, M.W., Peery, J.S., and M.S. Ingber, "Velocity Boundary Conditions for Vorticity Formulations of the Incompressible Navier-Stokes Equations," SAND94-1735, 1995
- 16 Kinney, R. B., and M.A. Paolino, "Flow Transient Near the leading Edge of a Flat Plate Moving Through a Viscous Fluid," ASME J. Appl. Mech., vol 41, 1974
- 17 Korn, G. A. and T. M. Korn, <u>Mathematical Handbook for Scientists and Engineers</u>, McGraw-Hill, 2nd Edition, 1968
- 18 Koumoutsakos, P. and A. Leonard, "Improved Boundary Integral Method for Inviscid Boundary Condition Applications," AIAA Journal, vol. 31, no. 2, pp. 401-4041993
- 19 Koumoutsakos, P., Leonard, A., and F. Pepin, "Boundary Conditions for Viscous Vortex Methods," *Journal of Computational Physics*, vol. 113, pp. 52-61, 1994.
- 20 Koumoutsakos, P. and A. Leonard, "High-Resolution Simulations of Flow around an imputlsively started cylinder using Vortex Methods," J. Fl. Mech., vol. 296, pp. 1-38, 1995.
- Leonard, A., "Vortex Methods for Flow Simulation," J. Comput. Phys., vol. 37, pp. 289-355, 1980.
- 22 Leonard, A., "Computing Three-Dimensional Incopressible Flows iwth Vortex Elements," An. Rev. Fluid Mech., vol. 17, pp. 523-559, 1985.
- 23 Lyman, F. A., "Vorticity Production at a Solid Boundary," in Some Unanswered Questioned in Fluid Dynamics, ASME publication 89-WA/FE-5, 1989.
- Lighthill, M. J., "Chapter II. Introduction: Boundary Layer Theory," in <u>Laminar Boundary Layers</u>, Rosenhead, L., Editor, Oxford at the Clarendon Press, 1963.
- 25 Meir, A. J. and P. G. Schmidt, "Variational mehtods for Stationary MHD Flow Under Natural Interface Conditions," To Appear, *J. Non-Linear Analysis*, 1996.
- 26 Mihklin, S. G., Integral Equations and Their Applications to Certain Problems of Mechanics, 2nd Ed. MacMillan, Neew York, 1964.
- 27 Morino, L., "Helmholtz Decomposition Revisited: Vorticity Generation and Trailing Edge Condition," *Computational Mechanics*, vol. 1, pp. 65-90, 1986.
- Morino, L., "Boundary Integral Equations in Aerodynamics," *Applied Mechanics Reviews*, vol. 46, no. 8, pp. 445,-466, August 1993.
- 29 Morse, P.M. and H. Feshback, <u>Methods of Theoretical Physics</u>, Part II, McGraw-Hill Publ. Co., 1953.

- Ostrikov, N. N. and E. M. Zhmulin, "Vortex Dynamics of Viscous Fluid Flows: Part1. Two-Dimensional Flows," F. Fl. Mech., vol. 276, pp. 81-111, 1994.
- Parmentier, E.M. and K.E. Torrance,"Kinematically Consistent Velocity Fields for Hydrodynamic Calculations in Curvilinear Coordinates," *J. Comput. Phys.*, vol. 19, 404-417, 1975.
- Puckett, E. G., "Vortex Methods: An Introduction and Survey of Selected REsearch Topics," in <u>Incompressible Computational Fluid Dynamics</u>, edited by M.D. Gunzburger and R. A. Nicolaides, Cambridge University Press, 1993.
- Quartapelle, L., "Vorticity Conditioning in the Computation of Two-dimensional Viscous Flows, J. Comput. Phys., vol. 40, pp. 453-477, 1981.
- Quartapelle, L. and F. Valz-Gris, "Projection Conditions on the Vorticity in Viscous Incompressible Flows," *International Journal for Numerical Methods in Fluids*, vol. 1, pp. 129-144, 1981.
- 35 Roache, P., Computational Fluid Dynamics, Hermosa Press, 1972.
- 36 Sarpkaya, T., "Vortex Element Methods for Flow Simulation," Advances in Applied Mechanics, vol. 31, p. 131, 1994.
- 37 Uhlman and Grant, "A New Method for the Implementation of Boundary Conditions in the Discrete Vortex Element Method," ASME 1993 Fluids Engrg. Sprg. Mtg., Wash., D.C., June 1993.
- Weatherburn, C.E., Differential Geometry of Three Dimensions, Cambridge Universtiy Press, 1939.
- Wu, J. C. and J. F. Thompson, "Numerical Solutions of Time-Dependent Incompressible Navier-Stokes Equations Using an Integro-Differential Formulation," Computers & Fluids, vol. 1, pp. 197-215, 1973.
- Wu, J. C., "Numerical Boundary Conditions for Viscous Flow Problems," AIAA Journal, vol. 14, pp. 1042-1047, 1976.
- Wu, J. C. and U. Gulcat, "Separate Treatment of Attached and Detached Flow Regions in General Viscous Flows," AIAA Journal, vol. 19, no. 1, pp. 20-27, 1981.
- Wu, J. C., "Boundary Elements and Viscous Flows," pp. 3-18, <u>Boundary Element Technology VII</u>, Computational Mechanics Publications, co-published with Elsevier Applied Science, 1992, Edited by C. A. Brebbia and M. S. Ingber.
- 43 Wu, J.-Z., Wu X., Ma, H., and J. Wu, "Dynamic Vorticity Condition: Theoretical Analysis and Numerical Implementation," *International Journal for Numerical Methods in Fluids*, vol. 19, pp. 905-938, 1994.

Wu, X. H., J.Z. Wu, and J. M. Wu, "Effective Vorticity-Velocity Formulations for Three-Dimensional Incompressible Visocus Flows," J. Comput. POhys., vol. 122, pp. 68-82, 1995.

Distribution

Analytical Methods (2) P.O. Box 3786 Bellevue, WA 98009 Attn: F. Dvorak B. Maskew

Mr. James Fein Code 1221 ONR 800 N. Quincy St. Arlington, VA 22217

Dr. H. Higuchi Mech. Eng. & Aero. Dept Syracuse University Syracuse, NY 13244

Prof. Joseph Katz
Dept. Aerospace Eng. and Eng. Mech.
San Diego State University
San Diego, CA 92115

Dr. George A. Keramidas Code 4420 NRL Washington, DC 20375

Prof. A. Leonard Graduate Aeronautics Lab. California Institute of Technology Pasadena, CA 91125

Prof. M. Luttges Dept. of Aerospace Eng. Sci. University of Colorado Boulder, CO 80309-0429

Dr. R. C. Maydew 5305 Queens Ct. NE Albuquerque, NM 87109

Prof. R. N. Meroney Dept. of Civil Eng. Colorado State University Fort Collins, CO 80521 NASA Johnson Space Center (2) Attn: EG3 Houston, TX 77058 Attn: D. B. Kanipe R. E. Meyerson

New Mexico State University (2) Dept. of Mech. Eng. Las Cruces, NM 88003 Attn: Ron Pederson G. Reynolds

Mr. W. J. Quinlan Aerodynamic Design Ford Motor Company 21175 Oakwood Blvd. Dearborn MI, 48123

Prof. T. Sarpkaya
Dept. Mech. Eng.
Code 69-SL
Naval Postgraduate Academy
Monterey, CA 93943

Prof. Roger L. Simpson
Dept. Aerospace and Ocean Eng.
Virginia Polytechnic Institute
and State University
Blacksburg, VA 24061

Mr. J. T. Strickland Sterling Chemical Co. Post Office Box 1311 Texas City, TX 77592

Texas Tech University (2)
Dept. of Mech. Eng.
Lubbock, TX 79409
Attn: J. H. Lawrence
J. W. Oler

University of New Mexico (2)
Dept. of Mech. Eng.
Albuquerque, NM 87106
Attn: M. S. Ingber
C. R. Truman

- MS 0320 1011 C. E. Meyers
- MS 0841 9100 P. J. Hommert
- MS 0835 9102 R. D. Skocypec
- MS 0826 9111 W. L. Hermina
- MS 0826 9111 C. E. Hickox
- MS 0826 9111 P. R. Schunk
- MS 0827 9111 M. A. Christon
- MS 0826 9111 S. N. Kempka (15)
- MS 0826 9111 M. W. Glass (5)
- MS 0834 9112 A. C. Ratzel
- MS 0834 9112 J. R. Torczynski
- MS 0833 9116 C. W. Peterson
- MS 0833 9116 J. H. Strickland (15)
- MS 0835 9116 S. Tiesczen
- MS 0704 6201 P. C. Klimas
- MS 0708 6214 H. M. Dodd
- MS 0708 6214 D. E. Berg
- MS 9051 8351 W. T. Ashurst
- MS 0411 9723 J. M. Macha
- MS 0105 9835 R. B. Asher
- 1 MS 9018 Central Tech Files, 8523-2
- 5 MS 0899 Technical Library, 4414
- 1 MS0619 Print Media, 12615
- 2 MS 0100 Doc.Proc.DOE/OSTI, 7613-2(10)